Bioorganic & Medicinal Chemistry 22 (2014) 2280–2293

Contents lists available at ScienceDirect

Bioorganic & Medicinal Chemistry

journal homepage: www.elsevier.com/locate/bmc

Discovery of 3-(4-methanesulfonylphenoxy)-*N*-[1-(2-methoxy-ethoxymethyl)-1*H*-pyrazol-3-yl]-5-(3-methylpyridin-2-yl)-benzamide as a novel glucokinase activator (GKA) for the treatment of type 2 diabetes mellitus

Kaapjoo Park *, Byoung Moon Lee, Kwan Hoon Hyun, Dong Hoon Lee, Hyun Ho Choi, Hyunmi Kim, Wonee Chong, Kyeong Bae Kim, Su Youn Nam

Yuhan Research Institute, 25, Tapsil-ro 35beon-gil, Giheung-gu, Yongin-si, Gyeonggi-do, Republic of Korea

ARTICLE INFO

Article history:
Received 27 December 2013
Revised 5 February 2014
Accepted 9 February 2014
Available online 17 February 2014

Keywords:
Type 2 diabetes mellitus (T2DM)
Glucokinase activator (GKA)

ABSTRACT

Novel heteroaryl-containing benzamide derivatives were synthesized and screened using an in vitro assay measuring increases in glucose uptake and glucokinase activity stimulated by 10 mM glucose in rat hepatocytes. From a library of synthesized compounds, 3-(4-methanesulfonylphenoxy)-*N*-[1-(2-methoxy-ethoxymethyl)-1*H*-pyrazol-3-yl]-5-(3-methyl pyridin-2-yl)-benzamide (**19e**) was identified as a potent glucokinase activator with assays demonstrating an EC_{50} of 315 nM and the induction of a 2.23 fold increase in glucose uptake. Compound **19e** exhibited a glucose AUC reduction of 32% (50 mg/kg) in an OGTT study with C57BL/6J mice compared to 28% for metformin (300 mg/kg). Single treatment of the compound in C57BL/J6 and ob/ob mice elicited basal glucose lowering activity, while in a two-week repeated dose study with ob/ob mice, the compound significantly decreased blood glucose levels with no evidence of hypoglycemia risk. In addition, **19e** exhibited favorable pharmacokinetic parameters in mice and rats and excellent safety margins in liver and testicular toxicity studies. Compound **19e** was therefore selected as a development candidate for the potential treatment of type 2 diabetes.

1. Introduction

Hyperglycemia is a condition commonly caused by defects in the secretion or action of insulin, and triggers the development of diabetes mellitus. Chronic hyperglycemic conditions typical of diabetes are associated with macrovascular complications including coronary artery disease, peripheral arterial disease and stroke.[1] Diabetes can also cause microvascular complications such as diabetic retinopathy, nephropathy and neuropathy.

Type 2 diabetes mellitus (T2DM) now affects over 300 million people worldwide. Rates of diabetes have increased noticeably over the last 50 years with a concomitant trend in the increasing rates of obesity, which is thought to be a primary factor in its cause.[2] Although various anti-diabetic drugs are available (e.g., biguanides, α-glucosidase inhibitors, sulfonylureas, gliptins, TZDs, DPP-4 inhibitors, incretin mimetics (GLP-1 analogs) and newly approved SGLT2 inhibitors[3] (dapagliflozin[4] and canagliflozin[5])), these drugs are effective in reducing plasma glucose or glycated hemoglobin A1c (HbA1c), but monotherapy commonly results in treatment failure, leading to the need for combination therapy.[6] In addition, some drugs exhibit side effect profiles that include an increased risk of hypoglycemia (sulfonylureas, gliptins), GI complications (biguanides, α-glucosidase inhibitors), cardiovascular risk (TZDs), pancreatitis risk (DPP-4 inhibitors, incretin mimetics) and genital/urinary tract infections (SGLT2 inhibitors). Thus, there exist interrelated unmet needs in type 2 diabetes that include a better balance of efficacy of glycemic control with cardiovascular safety, improved durability of treatment, hypoglycemia avoidance, tolerability and ease of compliance.

Glucokinase (GK, also called hexokinase IV or hexokinase D) is a hexokinase isozyme composed of 465 amino acids (molecular weight = 50 kD). GK facilitates phosphorylation of glucose to glucose-6-phosphate, which comprises the first step of both glycogen synthesis and glycolysis. GK is expressed in cells of the liver,

Abbreviations: GK, glucokinase; GKA, glucokinase activator; SU, sulfonylurea; DPP-4, dipeptidyl peptidase-4; TZD, thiazolidinedione; SGLT2, sodium-glucose co-transporter 2; GSIS, glucose-stimulated insulin secretion; OGTT, oral glucose tolerance test; PK, pharmacokinetics; T2DM, Type 2 diabetes mellitus.

* Corresponding author. Tel.: +82 31 899 4274; fax: +82 31 275 6145.
E-mail address: kaapjoo@yuhan.co.kr (K. Park).

http://dx.doi.org/10.1016/j.bmc.2014.02.009
0968-0896/

pancreas, gut, and brain in humans and many other vertebrates. In comparison to other hexokinases, GK has a lower affinity for glucose and its activity is localized to only a few cell types. Partly as a result of this reduced affinity, GK activity varies substantially with the concentration of glucose present. Furthermore, unlike other hexokinases, GK is not inhibited by its product, glucose-6-phosphate[7] and distinctively, GK shows moderate cooperativity with glucose, with a Hill coefficient (n_H) of approximately 1.7.[8] Slow conformational changes between multiple interconverting states have been proposed to be responsible for this kinetic positive cooperativity.[9] Due to this moderate cooperativity, a half-saturation level $S_{0.5}$ (the concentration at which the enzyme is 50% saturated and active) is used for GK instead of using a K_m for glucose.[10] GK acts as a glucose sensor regulating hepatic glucose metabolism to provide approximately 95% of the hexokinase activity in hepatocytes[8] and GK activity serves as a key control for glucose-dependent insulin secretion in islet beta cells.[11] Glucokinase activator (GKA) is associated with a dual mechanism for lowering blood glucose concentrations by enhancing glucose uptake in the liver and increasing insulin secretion from pancreatic beta cells. Therefore, GK has been an attractive target for anti-diabetic therapy over the last two decades. Several GKA candidates have advanced to clinical studies and have been shown to lower both fasting and postprandial glucose levels in healthy subjects and T2DM patients. Hypoglycemia and liver or testicular toxicity[12] have been revealed as the primary adverse effects of concern for GKAs. To address the hypoglycemia issue, several clinical strategies have been utilized including dose titration and more frequent dosing times. Recently, two novel strategies have been employed to reduce the potential for hypoglycemic induction. One strategy is the design of partial activators that improve the dependence of enzymatic activity on various physiological glucose levels.[13] The other is to create liver-selective glucose activators[14–16] that restrict the main enzymatic activity in the liver, since hypoglycemia risk is postulated to result from increases in pancreatic insulin secretion at low glucose levels. Initially, we adopted a dose titration clinical strategy to reduce the possibility of hypoglycemia caused by GKA.[17,18] Later, we employed another strategy involving the monitoring of activation profiles of dose-dependent $S_{0.5}$, where the ideal $S_{0.5}$ could be higher than 2. Through this strategy, we could demonstrate control of the balance between the potency of GKA and its adverse effects including hypoglycemia and liver toxicity.

To address the testicular toxicity issue[12] that is presumably related to compound specificity, we performed 7-day tox screen testing in C57Bl/6J mice using high doses of the compounds. This approach led to the discovery of a potent GKA lead candidate with good efficacy and a desirable safety margin. There are arguments disputing the value of GK activation for the treatment of T2DM after two decades of attempts, that have occurred without medical success in GKA development.[19] However, several phase I studies have demonstrated that GKAs can normalize blood sugar in T2DM patients[20] and long-term GKA treatment prevents the development of diet-induced diabetes mellitus in mice.[21] Currently, several small molecule GKAs are in human clinical studies (phase I and II).

GK is also an attractive target for the treatment of T2DM due to its dual action resulting in hepatic and pancreatic effects. A number of allosteric small molecule GKAs have been investigated by numerous research groups over the past decade[22–24] (selected representative small molecule GKAs are shown in Fig. 1). Since the first report of small molecule allosteric GKAs in 2003,[25] a phenylacetamide series (**2**),[26] benzamides (**1**,[27] **4**–**7**[28–30,12]) and an imidazolylacetamide (**8**)[14] have also been identified as potent GKAs. A binding mode at an allosteric site of GK was revealed by researchers in 2009 through the formation of co-crystal structures of the GK–compound **1** complex[27] and other GK–GKA complexes.[31] Due to the valuable structural information generated from research into these complexes, it is now possible to rationally design compounds for further improvement of molecule-target binding motifs. GKAs hypothetically bind to the allosteric binding site of the protein to achieve anti-hyperglycemic effects. Various benzamide derivatives have been prepared based on binding mode analysis of the X-ray structure of the allosteric binding site of GK. More recently, Park, et al., identified a novel phenylethyl benzamide GKA (**9**)[17,18] which exhibits good biological and pharmacological activity with favorable pharmacokinetics. Herein, we report the discovery of a novel pyrazole benzamide glucokinase activator harboring 3-methylpyridine and 4-phenoxymethyl sulfone groups, as a promising preclinical candidate for the treatment of T2DM.

2. Results and discussion

2.1. Chemistry

The benzamide scaffold was chosen as a starting point for the synthesis of selective GKAs due to the existence of unambiguous structural information from the known co-crystal complexes. Initially, hundreds of benzamide derivatives with various different substituents around a central benzene ring were synthesized based on the binding mode hypothesis shown in Figure 2.

The A-region of the molecule is required to have both a hydrogen bond donor (NH) and a hydrogen bond acceptor (=N) in order to bind to Arg63 favorably. The B moiety is required to be of a small size with potential hydrophobic interactions occurring with Tyr214, Tyr215 and Leu451. The C-pocket of the enzyme is fairly large and the end portion of C-moiety has the potential for a hydrogen bonding interaction with Arg250 in order to increase binding affinity. Through initial diversification and structure–activity relationship (SAR) analysis, 3-methylpyridine and 4-phenoxymethyl sulfone groups have been identified as optimal moieties for the B-region and C- region, respectively. The A-region was then investigated systematically by introducing a variety of aryl or hetero-aromatic groups which led to the identification of thiazole and pyrazole groups by prioritizing compounds based on in vitro potency and physicochemical properties. The synthesis of compounds, thiazole benzamide derivatives and pyrazole benzamide derivatives is outlined in Scheme 1.

The reaction of 4-fluorophenyl methyl sulfone and methyl 3,5-dihydroxybenzoate in the presence of Cs_2CO_3 gave phenoxy phenol **10**. Triflation of phenoxy phenol **10** followed by boration of the resulting triflate afforded boron compound **11**. Pd-catalyzed coupling of **11** with 2-bromo-3-methylpyridine provided 2-(3-methyl pyridyl)-benzene methyl ester **12** in moderate yield. Hydrolysis of methyl ester **12** yielded benzoic acid **13**. The amide coupling reaction of **13** with ethyl 2-aminothiazole-4-acetate gave thiazole amide ethyl ester and hydrolysis of the resulting ethyl ester provided acid **14**. A subsequent amide coupling reaction of **14** with various amines afforded final amide products **15a**–**b**. An amide coupling reaction of acid **13** with 2-aminothiazole or 5-fluoro-2-aminothiazole, or 4-(chloromethyl)-2-aminothiazole produced thiazole amides **16a**, **16b**, and **17**, respectively. 4-(Chloromethyl)-thiazole amide **17** was further elaborated to generate a variety of aminomethyl thiazoles **18a**–**k** by using routine nucleophilic amine substitution reactions. In addition, benzoic acid **13** was coupled with various substituted pyrazoles that were prepared beforehand to make pyrazole amide derivatives **19a**–**e** as shown in Scheme 2. The prepared thiazole benzamides and pyrazole benzamides were tested using an in vitro assay by measuring fold increase of GK activity at 10 mM glucose concentration. The compounds that exhibited satisfactory

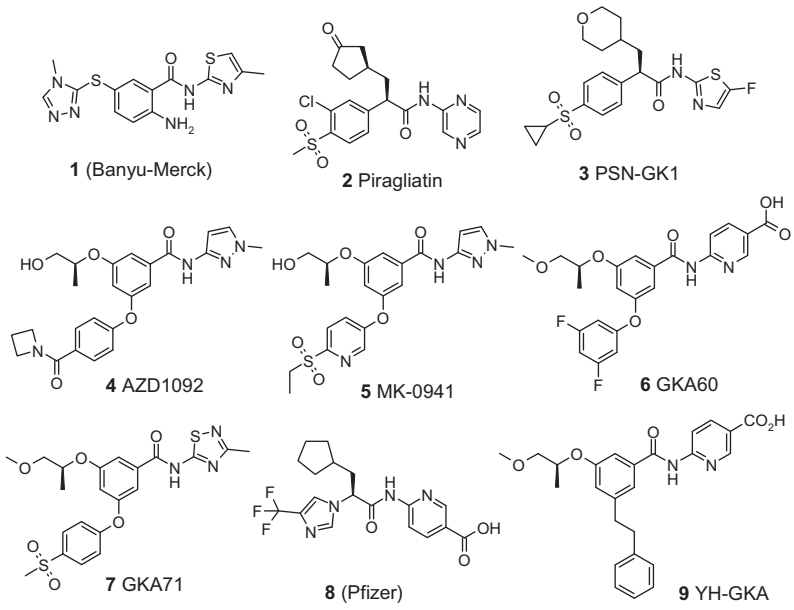

Figure 1. Representative structures of GKAs.

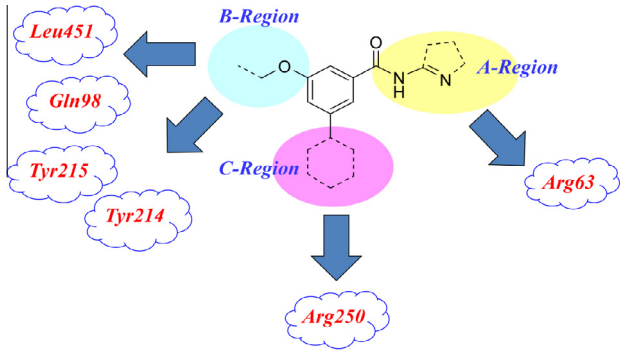

Figure 2. Binding mode hypothesis for benzamide GKAs.

enzyme activity were tested in a glucose uptake assay with hepatocyte cells. Subsequently, the selected compounds that demonstrated good glucose uptake activity were evaluated using an in vivo oral glucose tolerance test (OGTT). The biological results of thiazole amides, **16a**–**b** and **18a**–**k**, and pyrazole benzamides **19a**–**e** have been summarized in Tables 1 and 2.

2.2. Biological assays

An enzymatic glucokinase assay using purified recombinant human pancreatic glucokinase was used to evaluate the compounds. Selectivity against hexokinase I and II was tested using enzymatic assays. Glucose uptake assays using rat primary hepatocytes and an insulin secretion assay in Min6 cells or in rat pancreatic islets were performed to evaluate the effect of glucokinase activity on glucose-dependent insulin secretion. Anti-diabetic effects of selected compounds were evaluated using glucose tolerance tests in normal and diabetic db/db mice. To investigate efficacy with an oral glucose tolerance test (OGTT), eight-week old male C57BL/6 mouse (OrientBio Inc, Republic of Korea) and ten-week old male C57BLKS/J db/db mice (SLC Inc, Japan) were fasted overnight (with free access to water) before performing the test. The mice were orally administered with the compound or vehicle alone (0.5% methylcellulose solution).

2.3. Structure–activity relationships (SAR)

The biological activity data of selected thiazole benzamide derivatives have been summarized in Table 1. The introduction of a fluorine group at the R^2 position in the thiazole ring decreased the potency of the enzyme EC_{50} by 2.5-fold (**16b** vs **16a**). Thus, while the R^2 position in the thiazole ring was fixed with H, the R^1 position on the thiazole ring was systematically substituted with various acetyl amides and methyl amines. Cyclopropyl amide **15a** maintained similar potency to **16a** and ethyl amide **15b** showed a 19-fold increase in potency as compared with **16a**. Other acetyl amides containing large substituents at the amide position had a tendency to exhibit weak potency (unpublished data). For methylamine derivatives, the potency varied with substituent patterns. In particular, some alkyl amine moieties, as shown by compounds **18a**, **18f**, **18k**, decreased the potency significantly. However, other alkyl amines, **18b**–**c** and **18h**–**j**, exhibited similar enzyme potency to **16a**. Among the methyl amine derivatives, compound **18g** significantly improved the enzyme potency by 12-fold with an EC_{50} of 8 nM. The potency improvement appears to result from the electrostatic interaction with the pocket and/or the size effect of the moiety. Most of the active compounds in the GK enzyme assay showed good glucose uptake activity with >1.7 fold increase in the presence of 5.6 mM glucose, except for **18c**. The compounds that exhibited sub-micromolar EC_{50} values of GK activity and a higher than 1.7 fold increase in the glucose uptake assay were chosen for in vivo OGTT experiments. Among the compounds measured by in vivo OGTT, compound **16a** exhibited a 29.8% AUC reduction at 50 mg/kg. For pyrazole benzamide derivatives summarized in Table 2, the morpholine ethyl moiety (**19d**) and the methoxyethylmethoxy moiety (**19e**) at the R^1 position improved enzyme potency by 2-fold and 2.5-fold respectively, compared to the compound with $R^1 = CH_3$ (**19a**). Both compounds exhibited good glucose uptake activity with >2-fold increase. Compound **19e** was tested using in vivo OGTT and found to exhibit a 32.3% AUC reduction at 50 mg/kg. Therefore, compound **19e** was chosen for further studies including additional in vivo activity, a basal glucose lowering test, DMPK, and toxicity tests (Table 3).

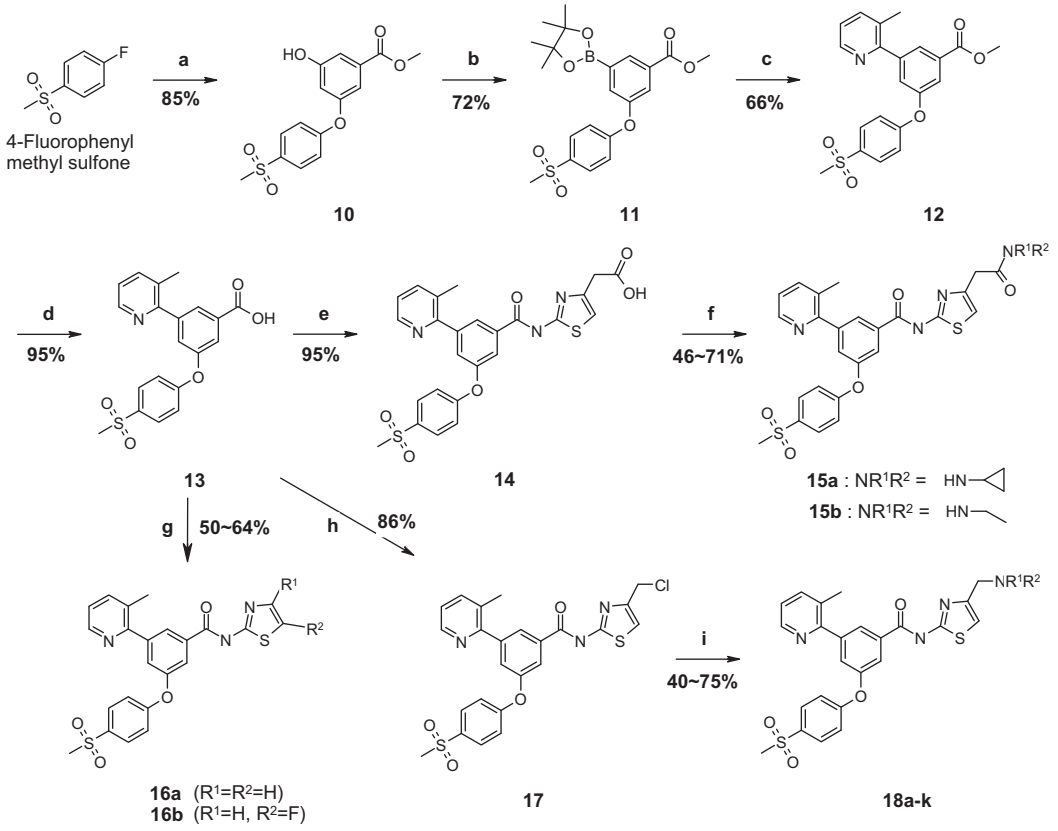

Scheme 1. Reagents and conditions: (a) Methyl 3,5-dihydroxybenzoate, Cs_2CO_3, DMF, reflux; (b) (i) Tf_2O, TEA, CH_2Cl_2, (ii) KOAc, $PdCl_2(dppf)$, Bis(pinacolato)diboron, 85 °C, 1,4-dioxane; (c) 2-bromo-3-methylpyridine, $Pd(PPh_3)_4$, Na_2CO_3, DMF/H_2O; (d) NaOH, THF/MeOH/H_2O; (e) (i) ethyl 2-aminothiazole-4-acetate, HOBT, EDAC, TEA, CH_2Cl_2, (ii) NaOH, THF/MeOH/H_2O; (f) R^1R^2NH, HOBT, EDAC, TEA, CH_2Cl_2; (g) 2-aminothiazole or 5-fluoro-2-aminothiazole, HOBT, EDAC, TEA, CH_2Cl_2; (h) (i) $SOCl_2$, reflux, (ii) 4-(chloromethyl)-2-thiazolamine, DIEA, CH_2Cl_2; (i) R^1R^2NH, K_2CO_3, KI, DMF.

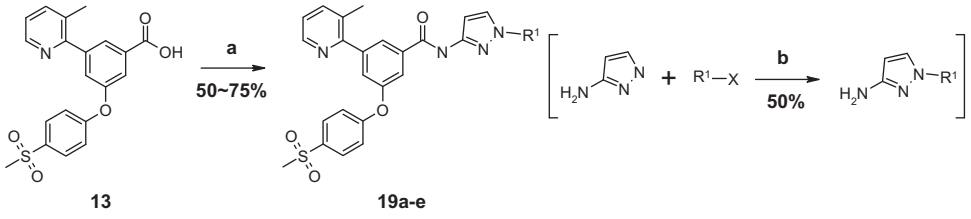

Scheme 2. Reagents and conditions: (a) 1-substituted 3-aminopyrazole, HOBT, EDAC, TEA, CH_2Cl_2; (b) K_2CO_3, DMF.

2.4. Molecular docking of 19e

To confirm the binding mode of glucokinase structure with diaryl benzamide derivatives, a crystal structure of glucokinase retrieved from RCSB Protein Data Bank (PDB entry code: 3A0I)[27] was used. A representative compound of 2-pyridinecarboxamide derivatives was co-crystallized with the binding site of glucokinase. The 3A0I-co-crystallized ligand showed good glucokinase potency (EC_{50} = 0.25 μM). According to analysis of the binding mode of the 3A0I-co-crystallized ligand, the 4-fluorophenylthio group occupied the binding pocket by eliciting hydrophobic interactions with Tyr214 and Gly97. The aminothiazole region exhibited preferable hydrogen bonding to Arg63.

To predict the binding mode of **19e** with the glucokinase structure, analysis with the Surflex-Dock program was conducted.[35] Compound **19e** docking conformers into the binding site of glucokinase were generated based on the scores. Total scores for the **19e** docked structure were 9.5, which represented a hydrogen bond, ionic, aromatic, and lipophilic interaction between the glucokinase and ligand. In addition, consensus scores represented by D_score, PMF_score, G_score and CHEM_socre were also validated. Consensus scoring integrated a number of popular scoring functions for ranking the affinity of ligands bound to the active site of the receptor. The highest scoring docked pose of **19e** structure is shown in Figure 3. According to binding mode analysis of the Surflex-Dock results, the aminopyrazole moiety elicited strong hydrogen bonds with Arg63 and the methyl-pyridine moiety was directed to the hydrophobic pocket surrounded by Tyr214, Tyr215 and Gly97. Methanesulfonyl phenoxy groups oriented toward the solvent exposed region with hydrogen bonding to Arg250. These critical interactions underscored the potent glucokinase activation potential of the **19e** ligand.

2.5. Biological activity of 19e

Pyrazole benzamide **19e** exhibited human pancreatic glucokinase activity of EC_{50} = 315 nM at 10 mM glucose with a half maximal saturation concentration ($S_{0.5}$) of 2.33 mM glucose and

Table 1
In vitro glucokinase activity of thiazole benzamide derivatives **15a–b**, **16a–b** and **18a–k**

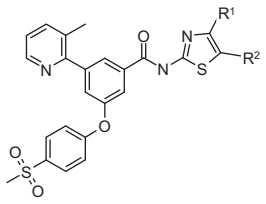

Compounds	R^1	R^2	$S_{0.5}$[a] (mM)	EC_{50}[b] at10 mM glucose, (μM)	Glucose uptake at 5.6 mM glucose, (fold)
16a	H	H	2.01	0.095	1.98
16b	H	F	1.95	0.238	1.75
15a	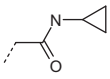	H	1.78	0.103	1.80
15b	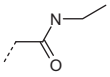	H	4.35	0.005	2.54
18a		H	5.79	>50	
18b	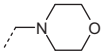	H	3.24	0.212	2.10
18c	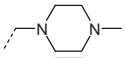	H	3.44	0.688	1.19
18d	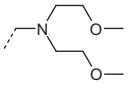	H	5.43	2.43	2.02
18e	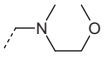	H	4.56	7.46	1.46
18f	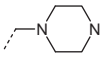	H	3.08	>50	
18g	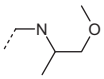	H	2.27	0.008	1.72
18h	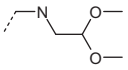	H	0.57	0.033	1.92
18i		H	3.98	0.463	1.47
18j	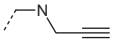	H	2.21	0.106	2.35
18k	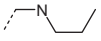	H	4.51	>50	

[a] Recombinant human pancreatic glucokinase was used and the activity was measured at 1 μM concentration.
[b] Data represented as the mean values of data obtained from three duplicate runs.

maximum reaction rate (V_{max}) of 150%. Treatment with **19e** also enhanced glucose uptake in rat primary hepatocytes by 2.23-fold and did not affect hexokinase I and II. The compound increased insulin secretion by 9-fold from MIN-6 cells and 3-fold from rat pancreatic islets in the presence of 11 mM glucose. It also improved oral glucose tolerance in C57BL/J6 mice in a dose-dependent manner (Fig. 4). An oral glucose tolerance test (OGTT) of **19e** at 50 mg/kg in C57Bl/6J mice revealed a blood glucose area under the curve (AUC) reduction of 32.3%, closely comparable to that of 29.9% for metformin at 300 mg/kg. As shown in Figure 4, compound **19e** showed no indication of hypoglycemia risk at 150 mg/kg. In addition, a combination of **19e** (50 mg/kg) and metformin (100 mg/kg) further increased the AUC reduction to 41.2%. In a two-week repeated dose study with db/db mice, **19e** showed significant decrease in blood glucose levels with 39.8% AUC reduction in OGTT (Fig. 5) and no adverse effects on serum lipid profiles or body weight.

It has been demonstrated that stimulators of insulin secretion (e.g., sulfonylureas, glinides, GKAs) can induce hypoglycemia. We therefore investigated the effect of **19e** on glucose lowering due to fasting without glucose challenge. Eight-week old male C57BL/6 mice (OrientBio Inc, Republic of Korea) were fasted for 6 h with free access to water, before being orally administered with the compound or vehicle alone (0.5% methylcellulose solution). Glucose levels were measured at 0, 30, 60, 90, 120, 180, 240, 300 and 360 min from the tail tip (Fig. 6). While sitagliptin, a DPP-4 inhibitor marketed by Merck & Co. under the trade name Januvia, has never been demonstrated to affect blood glucose levels under fasting conditions, **19e** exerted a glucose-lowering effect in the absence of glucose challenge. However, glucose levels after 60 min were maintained above 60 mg/dl, the minimum glucose level defined as non-hypoglycemic. GKA50, a potent GKA from AstraZeneca,[32] was used as a reference. These study results strongly support the notion that **19e** is a promising candidate for study in humans as a potential therapeutic agent for type 2 diabetes mellitus.

2.6. Physicochemical properties and pharmacokinetics of 19e

Compound **19e** possesses good aqueous solubility at 122 μM in phosphate buffer (pH 7.4) and a PAMPA permeability score of 2.62

Table 2
In vitro glucokinase activity of pyrazole benzamide derivatives **19a–e**

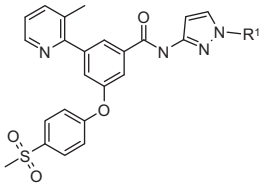

Compounds	R^1	$S_{0.5}$[a] (mM)	EC_{50}[b] at 10 mM glucose, (μM)	Glucose uptake at 5.6 mM glucose, (fold)
19a	CH_3	3.89	0.807	1.74
19b			>50	
19c	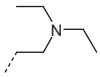		>50	
19d	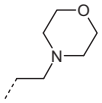	3.54	0.441	1.86
19e	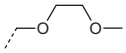	2.33	0.315	2.23

[a] Recombinant human pancreatic glucokinase was used and the activity was measured at 1 μM concentration.
[b] Data represented as the mean values of data obtained from three duplicate runs.

Table 3
In vivo OGTT results for the selected benzamide derivatives

Compounds	OGTT at 50 mg/kg, (AUC reduction, %)
16a	29.8**
16b	22.6**
15a	−3.1
15b	−0.3
18c	4.4
18d	20.2**
18i	2.2
19a	24.1**
19d	17.8*
19e	32.3**

Sample size = 6; significantly different from the vehicle-treated control *p <0.05 and **p <0.01.

(P_e 10^{-6} cm/s). In vitro metabolism studies for CYP inhibition and CYP induction were conducted using human liver microsomes and a PXR reporter gene assay. Metabolic stability studies were also performed using liver microsomes from mouse, dog and human. The pharmacokinetics of **19e** in mice and rats was determined following single intravenous and oral administration (Table 4).

Compound **19e** showed acceptable metabolic stability across species with more than 60% of the compound remaining after 1 h incubation. In vitro CYP inhibition (CYP1A2, 2B6, 2C8, 2C19, 2D6, 3A) and CYP induction (CYP3A4) studies for **19e** suggested no inhibitory effect except for 2C9 (IC_{50} = 5.2 μM) with no induction effect up to 25–50 μM concentration. Time-dependent inhibition (TDI) studies for **19e** were performed using human liver microsomes and no TDI was observed. Pharmacokinetic studies of **19e** in mice (Table 4) showed that the volume of distribution at steady state (V_{dss}) was 0.18 L/kg, elimination half-life ($t_{1/2}$) was 1.4 h, and bioavailability (F) was 24%. Overall, **19e** exhibited moderate bioavailability and a relatively short half-life in mice. However these PK data might support a b.i.d. (twice daily) or t.i.d. (three times daily) prescription strategy for GKA in humans to control postprandial glucose levels effectively and to avoid possible hypoglycemic risk. In vitro examination of CYP inhibition/induction and PK results suggested that **19e** has a low risk of drug–drug interactions in humans and a highly attractive pharmacokinetic profile for an oral anti-diabetic agent.

2.7. Toxicity evaluation of 19e

Since Waring et al., recently reported that GKAs containing pyridine-5-carboxylic acid (e.g., GKA60 (**6**) and GKA50) might cause testicular toxicity,[12] we carefully monitored organ toxicity for our GKA compounds. To address the testicular toxicology liability during the optimization of GKA compounds, we developed a 7-day tox screen assay using high doses of compounds (normally 300 and 500 mg/kg) and found that testicular toxicity might be related to the structure of compounds based on assessment of the results. An oral dose toxicity study was carried out in rats to evaluate the testicular toxicity of **19e** when administered daily via oral gavage to rats for 14 days (Table 5). The dose dependent increase of systemic exposures of **19e** was observed in the dose range of 250 to 1000 mg/kg in rats. The systemic exposure of **19e** was generally increased less than dose-proportionally in the dose range of 250–1000 mg/kg in both sexes on Day 1 and Day 14. No consistent sex differences were observed in systemic exposure and no accumulation of **19e** was observed in all dose groups in both sexes. The systemic exposure of **19e** after repeated dose was generally decreased in the 500 and 1000 mg/kg dose groups.

Assessment of toxicity was based on observations for mortality, clinical signs, body weight and food consumption data, clinical pathology, organ weights and macroscopic/microscopic examinations. Under the conditions of the current study, administration of **19e** was well tolerated to 1000 mg/kg and no test article-related toxicity findings were observed in any other organs.

For the histopathological examination of GKAs, test article-related microscopic findings included seminiferous tubule degeneration, seminiferous tubule vacuolation, and multinucleated giant cells in the testis. No test article-related microscopic findings for **19e** were observed in the testis of the high-dose group in this study. An escalating oral gavage dose range-finding study was performed to evaluate the potential testicular and liver toxicity of **19e** when administered in a repeated escalating-dose program (i.e., repeated doses of 100, 300, and 1000 mg/kg on Days 1, 4, and 7,

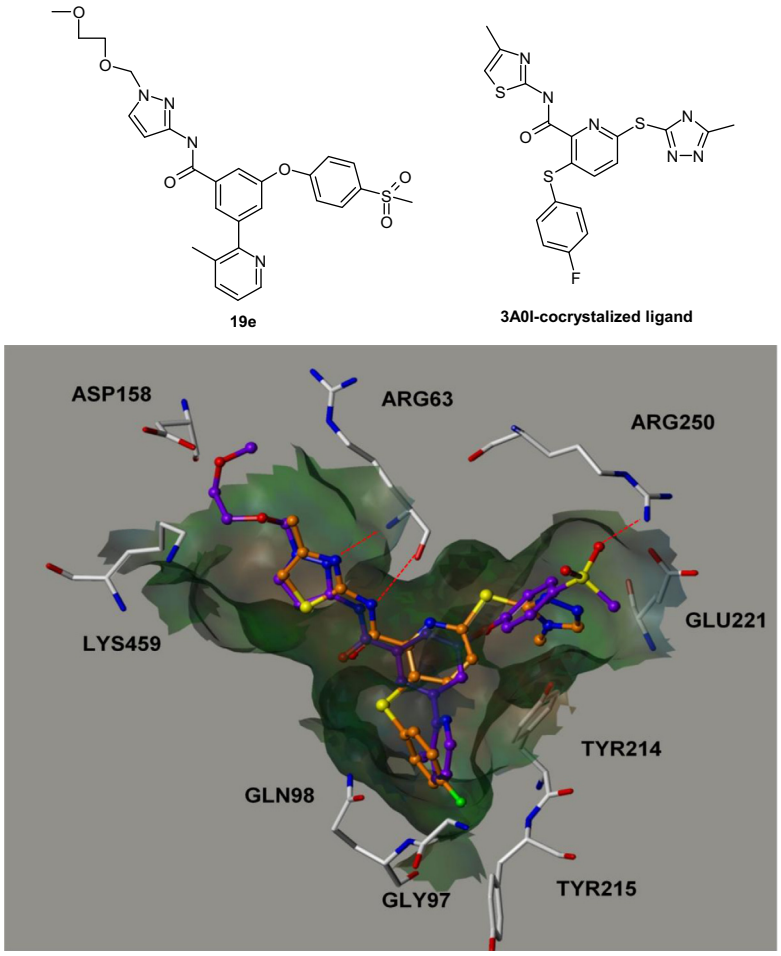

Figure 3. The docked conformer of **19e** (purple color based carbon type) at the active site of glucokinase as generated by Surflex-Dock, compared with the X-ray structure of 3A0I-co-crystallized ligand (orange color-based carbon type). Specific binding of **19e** to glucokinase shows potential hydrogen bonds in red dotted lines.

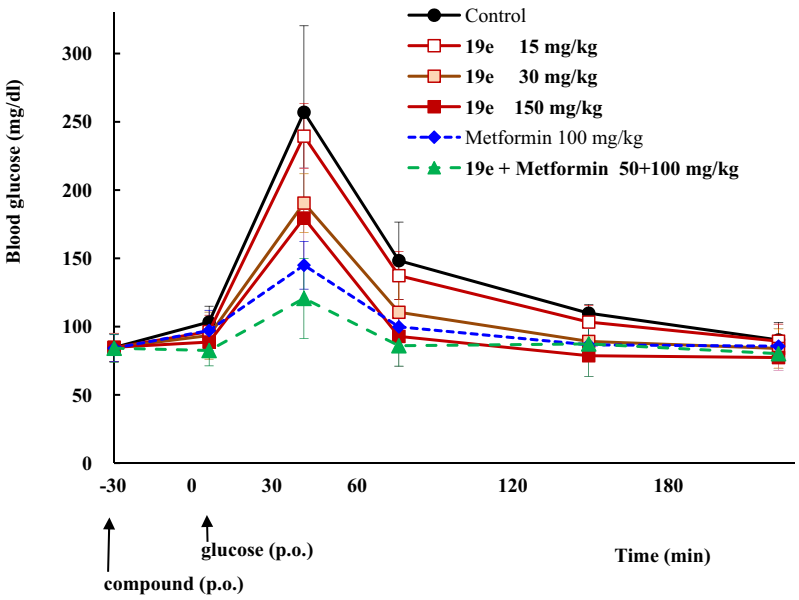

Figure 4. Plasma blood glucose lowering effect of **19e** in C57BL/J6 mice OGTT. (po: per os (oral administration); no of animals = 6; error bars represent standard deviation).

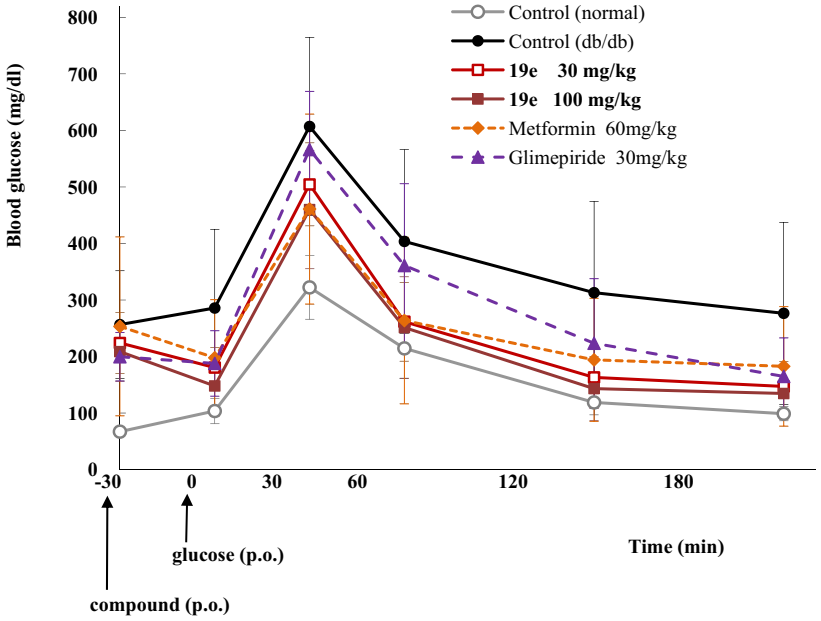

Figure 5. Plasma blood glucose lowering effect of **19e** in db/db mice OGTT. (po: per os (oral administration); no of animals = 6; error bars represent standard deviation).

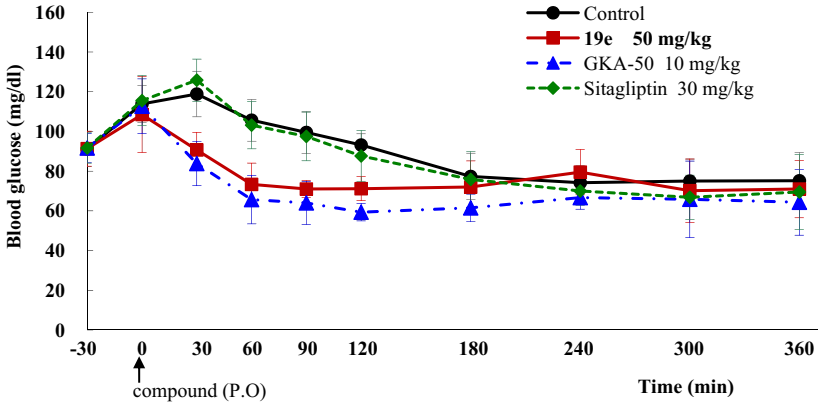

Figure 6. Glucose lowering activity of **19e** in C57BL/J6 mice in fasting conditions (no of animals = 6; error bars represent standard deviation).

Table 4
PK parameters of **19e** in mouse and rat

Species	Clearance (L/h/kg)	V_{dss} (L/kg)	MRT (h)	$T_{1/2}$ (h)	AUC (μg h/mL)	C_{max} (μg/mL)	T_{max} (h)	F (%)
Mouse	0.20	0.18	0.92	1.4	11.9	11.7	0.25	24
Rat	0.59	0.21	0.37	0.3	3.8	3.7	0.42	22

Table 5
Mean toxicokinetic parameter of **19e** on Day 1 and Day 14 after oral administration of **19e** for 14 days at the dose levels of 250, 500 and 1000 mg/kg in rats

Parameter	Sex	Male			Female		
	Dose	250 mg/kg	500 mg/kg	1000 mg/kg	250 mg/kg	500 mg/kg	1000 mg/kg
C_{max}	Day1	3055	4100.3	4250.3	3451.3	4297.7	7590.7
(ng/mL)	Day 14	1816.3	2795.5	3093.7	5201.3	3917.3	5213.0
T_{max}	Day1	2.7	3.7	4.0	3.7	3.3	2.7
(h)	Day 14	3	3	5	1.3	1.3	2.7
AUC_{0-t}	Day1	13145.8	16934.7	35445.8	13727.9	19750.3	29243.1
(ng h/mL)	Day 14	8177.6	13593.8	25043.8	17567.2	16293.9	23978.8

respectively) via oral gavage to beagle dogs for 8 days. No test article-related microscopic findings for **19e** were observed in the testis.

A mutagenicity study was carried out according to standard Ames test procedures (Maron and Ames). Two different *Salmonella typhimurium* strains (TA98 and TA100) were used in the reverse mutation test both in the presence and absence of S9 mix. Cytotoxicity caused by **19e** was not observed at all dose levels and there were no increases in revertants per plate at any dose level for the TA98 and TA100 strains in the presence and absence of S9 mix (please see the Section 4). Taken together, these bacterial assay results suggest that **19e** is not mutagenic.

3. Conclusion

Various benzamide derivatives have been synthesized by modifying three main regions around a benzamide scaffold. Lead optimization led to the identification of 3-methylpyridine and 4-phenoxymethyl sulfone groups as optimal moieties for the B-region and C-region, respectively. Consequently, the A-region was optimized to identify thiazole and pyrazole groups as optimal moieties in terms of in vitro potency and physicochemical properties. Among the thiazole and pyrazole benzamide derivatives, Compound **19e** was found to be an active GKA with an EC_{50} of 315 nM and induced a glucose reduction of 32.3% (50 mg/kg) in an OGTT study, equivalent to 300 mg/kg metformin. Single treatment in C57BL/J6 and db/db mice elicited basal glucose lowering activity. In addition, **19e** exhibited favorable bioavailability and an appropriate half-life for a b.i.d or t.i.d dosing strategy. More importantly, **19e** exhibits a good safety profile without any evidence of mutagenicity or liver/testicular toxicity.

In conclusion, the pyrazole benzamide GKA **19e** is a promising preclinical lead candidate with good efficacy and an excellent safety profile, with low risk hypoglycemic risk for the treatment of T2DM. To further improve the efficacy and safety profile with additional benefits, the lead optimization of a novel GKA scaffold is continuing with an innovative and translational screening strategy.

4. Experimental

4.1. Chemistry

All reagents and solvents were used as received from commercial sources. ^{1}H NMR spectra were recorded on a Bruker, Avance 400 Spectrometer 400 MHz nuclear magnetic resonance spectrometer. ^{1}H NMR spectra were recorded in $CDCl_3$, CD_3OD, or DMSO-d_6, and chemical shifts are reported relative to a TMS internal standard to the residual solvent peak (abbreviation in spectra: s = singlet, d = doublet, t = triplet, q = quartet, quin = quintet, m = multiplet). High-resolution mass spectra (HRMS) were obtained on a Waters Q-TOF Premier machine using electrospray ionization (ESI). Purity of all final analogues for biological testing were confirmed to be >95% as determined by UPLC analysis and inspection of NMR spectra. UPLC analysis was performed using an Acquity UPLC BEH○R C18 (1.7 μm, 2.1 × 100 mM) with 5% acetonitrile in water (0–1 min), 15–90% acetonitrile in water (1–8.5 min), 90% acetonitrile (8.5–10 min), with both solvents containing 0.1% formic acid as a modifier with a flow of 0.4 mL/min; and UV detection at 230 nM. Purification by flash chromatography was carried out using either Zeochem C-gel 560 (0.060–0.200 mM, Zeochem) or MPLC with a Teledyne Isco CombiFlash Rf with RediSep Flash columns using a gradient of ethyl acetate in *n*-hexanes or methanol in CH_2Cl_2, or similar instrument or reverse phase preparative HPLC. TLC analysis was performed on silica gel 60 F_{254} plates. Elemental analysis for carbon, hydrogen and nitrogen (CHN analysis) was accomplished by combustion analysis.

4.1.1. 3-Hydroxy-5-(4-methanesulfonylphenoxy) benzoic acid methyl ester (10)

To a solution of methyl 3, 5-dihydroxybenzoate (20.5 g, 0.13 mol) in DMF (130 mL) were added 4-fluorophenylmethyl sulfone (21.2 g, 0.12 mol) and cesium carbonate (59.3 g, 0.18 mol). The reaction mixture was heated at 180 °C for 3 h. The mixture was cooled to room temperature, and then water was added to the mixture. The reaction mixture was filtered through Celite pad and washed with ethyl acetate. The filtrate was extracted with ethyl acetate and the combined organic layers were washed with brine, dried over $MgSO_4$, and concentrated under reduced pressure. The residue was purified by flash column chromatography (EA/Pet.Ether = 1:5 ∼ 1:1) to afford 11.6 g (85% yield) of **10** as a white solid. ^{1}H NMR (400 MHz, $CDCl_3$) δ 7.91–7.89 (d, J = 8.8 Hz, 2H), 7.42 (s, 1H), 7.28–7.26 (m, 1H), 7.12–7.10 (d, J = 8.8 Hz, 2H), 6.80–6.79 (t, J = 4.0 Hz, 1H), 3.90 (s, 3H), 3.08 (s, 3H); TLC R_f 0.50 (50% EtOAc in petroleum ether).

4.1.2. 3-(4-Methanesulfonylphenoxy)-5-(4,4,5,5-tetramethyl-[1,3,2]dioxaborolan-2-yl) benzoic acid methyl ester (11)

To a solution of **10** (11.5 g, 0.036 mol) in dichloromethane (150 mL) were added trifluoromethanesulfonic anhydride (11.5 mL, 0.054 mol) and triethylamine (12.3 mL, 0.089 mol) at −78 °C bath. The reaction mixture was stirred for 2 h at −78 °C and then at room temperature overnight. The mixture was washed with saturated NH_4Cl aqueous solution and washed with brine. The organic layer was dried over $MgSO_4$, filtered, and concentrated under reduced pressure. The residue was purified by flash column chromatography (EA/Pet.Ether = 1:8 ∼ 1:4) to yield 14.0 g (86% yield) of 3-(4-methanesulfonylphenoxy)-5-trifluoromethanesulfonyloxy benzoic acid methyl ester as a white solid. ^{1}H NMR (400 MHz, $CDCl_3$) δ 7.99–7.97 (q, J = 8.0 Hz, 2H), 7.77–7.73 (m, 2H), 7.23–7.21 (m, 1H), 7.18–7.16 (d, J = 8.8 Hz, 2H), 3.95 (s, 3H), 3.09 (s, 3H); TLC R_f 0.60 (50% EtOAc in petroleum ether).

To a mixture of [1,1′-bis(diphenylphosphino) ferrocene]dichloropalladium (ll) (724 mg, 0.88 mmol), KOAc (5.8 g, 59.1 mmol) and bis(pinacolato) diboron (11.2 g, 44.3 mmol) in 1,4-dioxane (200 mL) was added 3-(4-methanesulfonylphenoxy)-5-trifluoromethanesulfonyloxy benzoic acid methyl ester (13.4 g, 29.5 mmol) at room temperature under nitrogen. The reaction mixture was heated at 85 °C overnight before it was cooled to room temperature, washed with saturated NH_4Cl aqueous solution, and extracted with ethyl acetate. The combined organic layer was washed with brine, dried over $MgSO_4$, filtered, and concentrated under reduced pressure. The residue was purified by flash column chromatography (EA/Pet.Ether = 1:12 ∼ 1:5) to yield 11.6 g (91% yield) of **11** as a pale yellow solid. ^{1}H NMR (400 MHz, $CDCl_3$) δ 8.33 (s, 1H), 7.90–7.88 (q, J = 4.8 Hz, 2H), 7.83–7.82 (m, 1H), 7.69 (s, 1H), 7.08–7.05 (d, J = 8.8 Hz, 2H), 3.70 (s, 3H), 3.06 (s, 3H), 1.35 (s, 12H); TLC R_f 0.50 (50% EtOAc in petroleum ether).

4.1.3. 3-(4-Methanesulfonyl-phenoxy)-5-(3-methyl-pyridin-2-yl)-benzoic acid methyl ester (12)

To a solution of **11** (11.5 g, 26.6 mmol) in DMF (100 mL) were added 2-bromo-3-methylpyridine (5.9 g, 34.58 mmol), tetrakis(triphenylphosphine) palladium (1.53 g, 1.33 mmol) and sodium bicarbonate (8.4 g, 79.8 mmol) in water (10 mL). The reaction mixture was heated at 80 °C for 18 h. The mixture was cooled to room temperature, diluted with water, and extracted with ethyl acetate. The combined organic layers were washed with brine, dried over $MgSO_4$, filtered, and concentrated under reduced pressure. The residue was purified by flash column chromatography (EA/

Pet.Ether = 1:5 ~ 1:2) to afford 7.0 g (66% yield) of **12** as a yellow solid. ^{1}H NMR (400 MHz, $CDCl_3$) δ 8.53–8.52 (d, J = 8.8 Hz, 1H), 8.09 (s, 1H), 7.93–7.91 (q, J = 4.8 Hz, 2H), 7.77–7.77 (m, 1H), 7.69–7.61 (m, 1H), 7.48–7.44 (m, 1H), 7.25–7.22 (m, 1H), 7.18–7.15 (m, 2H), 3.93 (s, 3H), 3.06 (s, 3H), 2.38 (s, 3H); TLC R_f 0.40 (50% EtOAc in petroleum ether).

4.1.4. 3-(4-Methanesulfonylphenoxy)-5-(3-methylpyridin-2-yl) benzoic acid (13)

To a solution of **12** (7.0 g, 17.6 mmol) in tetrahydrofuran (40 mL) and methanol (40 mL) was added NaOH (2.1 g, 52.9 mmol) in water (40 mL) and the reaction mixture was stirred at room temperature overnight. The reaction mixture was then concentrated under reduced pressure, diluted with water, acidified by 1 N HCl aqueous solution to pH = 6, and extracted with dichloromethane. The combined organic layers were dried over $MgSO_4$, filtered, and concentrated to afford 7.0 g (95% yield) of **13** as a pale white solid. ^{1}H NMR (400 MHz, $CDCl_3$) δ 8.52–8.50 (q, J = 5.2 Hz, 1H), 7.99 (s, 1H), 7.52–7.50 (m, 3H), 7.77–7.75 (q, J = 8.8 Hz, 1H), 7.65–7.60 (m, 3H), 7.57 (br s, 1H), 7.36–7.33 (m, 1H), 7.30–7.28 (m, 2H), 3.22 (s, 3H), 2.36 (s, 3H); TLC R_f 0.40 (5% MeOH in dichloromethane).

4.1.5. {2-[3-(4-Methanesulfonylphenoxy)-5-(3-methyl-pyridine-2-yl)-benzoylamino]-thiazol-4-yl}-acetic acid (14)

To a solution of **13** (3.7 g, 9.62 mmol) in dichloromethane (60 mL) were added ethyl 2-aminothiazole-4-acetate (1.97 g, 10.57 mmol), HOBT (1.49 g, 11.06 mmol), EDAC (2.11 g, 11.06 mmol) and triethylamine (2.47 g, 11.06 mmol) and the reaction mixture was stirred at room temperature overnight. The reaction mixture was then washed with 1 N HCl aqueous solution, saturated $NaHCO_3$ aqueous solution, and brine, before the organic layer was dried over $MgSO_4$, filtered, and concentrated under reduced pressure. The residue was purified by flash column chromatography (EA/Pet.Ether = 1:5 ~ 1:1) to afford 5.1 g (95% yield) of {2-[3-(4-methanesulfonylphenoxy)-5-(3-methyl-pyridine-2-yl)-benzoylamino]-thiazol-4-yl}-acetic acid ethyl ester as a white solid. TLC R_f 0.50 (5% MeOH in dichloromethane).

To a solution of {2-[3-(4-methanesulfonylphenoxy)-5-(3-methyl-pyridine-2-yl)-benzoylamino]-thiazol-4-yl}-acetic acid ethyl ester (4.0 g, 7.26 mmol) in THF (20 mL)/MeOH (20 mL) was added 3 N LiOH aqueous solution (7.26 mL, 21.78 mmol) and the reaction mixture was stirred at room temperature overnight. The reaction mixture was acidified by 1 N HCl aqueous solution to pH 6, The resulting solution was extracted with DCM and washed with brine. The organic layer was dried over $MgSO_4$, filtered and concentrated to yield 3.2 g (84% yield) of **14** as a yellow solid. ^{1}H NMR (400 MHz, DMSO) δ 12.63 (br s, 2H), 8.53–8.52 (d, J = 3.6 Hz, 1H), 8.20 (s, 1H), 7.99–7.92 (m, 3H), 7.79–7.77 (d, J = 7.6 Hz, 1H), 7.65–7.56 (m, 4H), 7.38–7.26 (m, 3H), 7.05 (s, 1H), 3.65 (s, 3H), 2.51 (s, 3H); TLC R_f 0.50 (10% MeOH in dichloromethane).

4.1.6. *N*-(4-Cyclopropylcarbamoylmethyl-thiazol-2-yl)-3-(4-methanesulfonyl-phenoxy)-5-(3-methyl-pyridine-2-yl)-benzamide (15a)

To a solution of **14** (100 mg, 0.19 mmol) in DCM (10 mL) were added cyclopropylamine (10.9 mg, 0.19 mmol), HOBT (29.6 mg, 0.23 mmol), EDAC (42.2 mg, 0.23 mmol) and triethylamine (49.3 mg, 0.29 mmol) and the reaction mixture was stirred at room temperature overnight. The reaction mixture was then washed with 1 N HCl aqueous solution, saturated $NaHCO_3$ aqueous solution, and brine. The organic layer was dried over $MgSO_4$, filtered, and concentrated under reduced pressure. The residue was purified by MPLC (MeOH/DCM = 5:95) to yield 75.9 mg (71% yield) of **15a** as a white solid. ^{1}H NMR (400 MHz, DMSO) δ 8.52–8.51 (d, J = 3.6 Hz, 1H), 8.18 (s, 1H), 8.04–8.03 (d, J = 4.0 Hz, 1H), 7.98–7.93 (m, 3H), 7.78–7.76 (d, J = 7.2 Hz, 1H), 7.59 (s, 1H), 7.37–7.30 (m, 3H), 6.95 (s, 1H), 3.43 (s, 2H), 3.22 (s, 3H), 2.62–2.60 (t, J = 7.2 Hz, 1H), 2.39 (s, 3H), 0.61–0.57 (m, 2H), 0.40–0.36 (m, 2H); HRMS (ESI-TOF) m/z for $C_{28}H_{27}N_4O_5S_2$ $[M+H]^+$ calcd 563.1423, found 563.1422; TLC R_f 0.50 (5% MeOH in dichloromethane). Anal. Calcd for $C_{28}H_{26}N_4O_5S_2$: C, 59.77; H, 4.66; N, 9.96. Found: C, 58.68; H, 4.67; N, 9.97.

4.1.7. *N*-(4-Ethylcarbamoylmethyl-thiazol-2-yl)-3-(4-methanesulfonyl-phenoxy)-5-(3-methyl-pyridine-2-yl)-benzamide (15b)

15b was prepared according to the procedure described for the synthesis of **15a** using ethylamine instead of cyclopropylamine. 46% yield, white solid. ^{1}H NMR (400 MHz, $CDCl_3$) δ 8.56 (s, 1H), 7.96–7.94 (d, J = 8.8 Hz, 2H), 7.72 (s, 1H), 7.67–7.65 (d, J = 6.4 Hz, 2H), 7.51 (s, 1H), 7.21–7.19 (m, 2H), 6.99 (s, 1H), 6.82 (s, 1H), 3.73 (s, 2H), 3.32–3.29 (t, 2H), 3.27–3.23 (m, 4H), 3.08 (s, 3H), 2.41 (s, 3H); HRMS (ESI-TOF) m/z for $C_{27}H_{27}N_4O_5S_2$ $[M+H]^+$ calcd 551.1423, found 551.1409. Anal. Calcd for $C_{27}H_{26}N_4O_5S_2$: C, 58.89; H, 4.76; N, 10.17. Found: C, 58.79; H, 4.79; N, 10.19.

4.1.8. 3-(4-Methanesulfonyl-phenoxy)-5-(3-methyl-pyridin-2-yl)-*N*-thiazol-2-yl-benzamide (16a)

To a solution of **13** (1.00 g, 2.6 mmol) in dichloromethane (20 mL) were added 2-aminothiazole (313 mg, 3.1 mmol), HOBT (705 mg, 5.2 mmol), EDAC (1000 mg, 5.2 mmol) and TEA (0.73 mL, 5.2 mmol) and the mixture was stirred overnight at room temperature. The reaction mixture was washed with 1 N HCl solution, washed with saturated $NaHCO_3$ solution, and brine. The organic layer was dried over $MgSO_4$, concentrated under reduced pressure and the residue was purified by flash column chromatography (EA/n-HX = 1:3 ~ 2:1) to yield 387 mg (32% yield) of **16a** as a white solid. ^{1}H NMR (400 MHz, $CDCl_3$) δ 11.46 (s, 1H), 8.55–8.54 (d, J = 4.0 Hz, 1H), 7.95–7.91 (m, 2H), 7.71–7.61 (m, 3H), 7.56–7.44 (m, 2H), 7.29–7.27 (m, 1H), 7.26–7.16 (m, 2H), 6.93–6.90 (m, 1H), 3.08 (s, 3H), 2.38 (s, 3H); HRMS (ESI-TOF) m/z for $C_{23}H_{20}N_3O_4S_2$ $[M+H]^+$ calcd 466.0895, found 466.0887; TLC R_f 0.38 (33% n-HX in EtOAc). Anal. Calcd for $C_{23}H_{19}N_3O_4S_2$: C, 59.34; H, 4.11; N, 9.03. Found: C, 59.25; H, 4.12; N, 8.99.

4.1.9. *N*-(5-Fluoro-thiazol-2-yl)-3-(4-methanesulfonyl-phenoxy)-5-(3-methyl-pyridin-2-yl)-benzamide (16b)

To a solution of **13** (228 mg, 0.59 mmol) in dichloromethane (5 mL) were added 5-fluoro-2-aminothiazole (184 mg, 1.19 mmol), HOBT (161 mg, 1.19 mmol), EDAC (228 mg, 1.19 mmol) and TEA (0.17 mL, 1.19 mmol) and the reaction mixture was stirred at room temperature overnight. The reaction mixture was then washed with 1 N HCl aqueous solution, saturated $NaHCO_3$ aqueous solution and brine. The organic layer was dried over $MgSO_4$, filtered and concentrated under reduced pressure, and purified by flash column chromatography (EA/n-Hex = 1:2 ~ 2:1) to yield 142 mg (50% yield) of **16b** as a yellow solid. ^{1}H NMR (400 MHz, $CDCl_3$) δ 11.39 (br s, 1H), 8.54–8.53 (d, J = 4.4 Hz, 1H), 7.98 (s, 1H), 7.91–7.89 (d, J = 9.2 Hz, 2H), 7.61–7.45 (m, 3H), 7.15–7.12 (d, J = 11.2 Hz, 2H), 6.91–6.90 (d, J = 2.8 Hz, 1H), 3.06 (s, 3H), 2.37 (s, 3H); HRMS (ESI-TOF) m/z for $C_{23}H_{19}FN_3O_4S_2$ $[M+H]^+$ calcd 484.0801, found 484.0788; TLC R_f 0.20 (33% n-HX in EtOAc). Anal. Calcd for $C_{23}H_{18}FN_3O_4S_2$: C, 57.13; H, 3.75; F, 3.93; N. Found: C, 57.08; H, 3.76; N, 3.96.

4.1.10. *N*-(4-Chloromethyl-thiazol-2-yl)-3-(4-methanesulfonyl-phenoxy)-5-(3-methyl-pyridine-2-yl)-benzamide (17)

Compound **13** (3.3 g, 8.60 mmol) was dissolved in $SOCl_2$ (10 mL), then the mixture was stirred at reflux for 1 h. The reaction

mixture was concentrated under reduced pressure to yield 3.46 g (100% yield) of yellow solid, which was used for the following step without further purification. To a solution of 3-(4-methanesulfonyl-phenoxy)-5-(3-methyl-pyridin-2-yl)-benzoyl chloride (3.46 g, 8.60 mmol) in DCM (50 mL) was added 4-(chloromethyl)-2-thiazolamine (1.75 g, 9.50 mmol) and *N*,*N*-diisopropylamine (6.67 g, 51.6 mmol) and the reaction mixture was stirred at room temperature overnight. The reaction mixture was washed with 1 N HCl aqueous solution, saturated $NaHCO_3$ aqueous solution, and brine. The organic layer was dried over $MgSO_4$, filtered and concentrated under reduced pressure, and purified by flash column chromatography (EA/Pet.Ether = 1:5 ~ 1:1) to afford 3.8 g (86% yield) of **17** as a brown solid. ^{1}H NMR (400 MHz, DMSO) δ 8.53–8.51 (d, J = 4.4 Hz, 1H), 8.20 (s, 1H), 7.98–7.95 (m, 3H), 7.79–7.77 (d, J = 7.6 Hz, 1H), 7.61 (s, 1H), 7.38–7.31 (m, 4H), 4.78 (s, 2H), 3.22 (s, 4H), 2.40 (s, 3H), 1.91 (s, 2H), 1.35 (s, 1H), 1.29–1.23 (m, 2H); HRMS (ESI-TOF) m/z for $C_{24}H_{27}ClN_3O_4S_2$ $[M+H]^+$ calcd 519.1052, found 519.1053; TLC R_f 0.50 (5% EtOAc in petroleum ether). Anal. Calcd for $C_{24}H_{26}ClN_3O_4S_2$: C, 56.08; H, 3.92; N, 8.17. Found: C, 55.98; H, 3.94; N, 8.20.

4.1.11. *N*-(4-Diethylaminomethyl-thiazol-2-yl)-3-(4-methanesulfonyl-phenoxy)-5-(3-methyl-pyridin-2-yl)-benzamide (18a)

To a solution of **17** (150 mg, 0.29 mmol) in DMF (5 mL) were added diethylamine (43 mg, 0.58 mmol), K_2CO_3 (54 mg, 0.58 mmol) and KI (4.8 mg, 0.03 mmol) and the reaction mixture was stirred at room temperature overnight. The reaction mixture was then washed with water and brine. The organic layer was dried over $MgSO_4$, filtered and concentrated under reduced pressure, and purified by MPLC (MeOH/DCM = 15:85) to afford 64 mg (42% yield) of **18a** as a white solid. ^{1}H NMR (400 MHz, $CDCl_3$) δ 8.48–8.47 (q, J = 4.8 Hz, 1H), 7.91–7.90 (m, 1H), 7.88–7.85 (m, 2H), 7.62–7.62 (t, J = 3.6 Hz, 1H), 7.58–7.56 (t, 1H), 7.43–7.42 (q, J = 7.6 Hz, 1H), 7.19–7.17 (m, 1H), 7.13–7.10 (m, 2H), 6.72 (s, 1H), 3.55 (s, 2H), 3.01 (s, 3H), 2.53–2.47 (dd, J = 7.6, 7.2 Hz, 4H), 2.34 (s, 3H), 1.00–0.96 (t, J = 14.4 Hz, 6H); HRMS (ESI-TOF) m/z for $C_{28}H_{31}N_4O_4S_2$ $[M+H]^+$ calcd 551.1786, found 551.1782. Anal. Calcd for $C_{28}H_{30}N_4O_4S_2$: C, 61.07; H, 5.49; N, 10.17. Found: C, 60.98; H, 5.47; N, 10.19.

The following compounds **(18b–k)** were prepared according to the procedure described above using suitable amines.

4.1.12. 3-(4-Methanesulfonyl-phenoxy)-5-(3-methyl-pyridin-2-yl)-*N*-(4-morpholin-4-ylmethyl-thiazol-2-yl)-benzamide (18b)

70% yield, white solid. ^{1}H NMR (400 MHz, $CDCl_3$) δ 8.51–8.49 (t, J = 4.8 Hz, 1H), 7.90–7.86 (m, 3H), 7.61–7.60 (q, J = 3.6 Hz, 1H), 7.58–7.56 (q, J = 8.4 Hz, 1H), 7.44–7.43 (q, J = 3.6 Hz, 1H), 7.20–7.18 (m, 1H), 7.13 (s, 1H), 7.11 (s, 1H), 6.74 (s, 1H), 3.66–3.64 (t, J = 9.2 Hz, 4H), 3.45 (s, 2H), 3.01 (s, 3H), 2.41–2.39 (t, J = 8.8 Hz, 4H), 2.34 (s, 3H); HRMS (ESI-TOF) m/z for $C_{28}H_{29}N_4O_5S_2$ $[M+H]^+$ calcd 565.1580, found 565.1586. Anal. Calcd for $C_{28}H_{28}N_4O_5S_2$: C, 59.56; H, 5.00; N, 9.92. Found: C, 59.48; H, 4.98; N, 9.96.

4.1.13. 3-(4-Methanesulfonyl-phenoxy)-*N*-[4-(4-methyl-piperazin-1-ylmethyl)-thiazol-2-yl]-5-(3-methyl-pyridin-2-yl)-benzamide (18c)

51% yield, brown solid. ^{1}H NMR (400 MHz, $CDCl_3$) δ 8.59–8.58 (d, J = 4.0 Hz, 1H), 8.08 (s, 1H), 7.96–7.94 (d, J = 8.4 Hz, 2H), 7.79 (s, 1H), 7.75–7.73 (d, J = 7.2 Hz, 1H), 7.54 (s, 1H), 7.35–7.35 (m, 1H), 7.22–7.20 (d, J = 9.2 Hz, 2H), 6.90 (s, 1H), 3.79(s, 2H), 3.17–3.10 (m, 3H), 3.08 (s, 2H), 3.02 (br s, 3H), 2.77 (s, 3H), 2.62 (s, 3H), 2.39 (s, 3H); HRMS (ESI-TOF) m/z for $C_{29}H_{32}N_5O_4S_2$ $[M+H]^+$ calcd 578.1896, found 578.1901. Anal. Calcd for $C_{29}H_{31}N_5O_4S_2$: C, 60.29; H, 5.41; N, 12.12. Found: C, 60.18; H, 5.43; N, 12.15.

4.1.14. *N*-(4-{[Bis-(2-methoxy-ethyl)-amino]-methyl}-thiazol-2-yl)-3-(4-methanesulfonyl-phenoxy)-5-(3-methyl-pyridin-2-yl)-benzamide (18d)

41% yield, white solid. ^{1}H NMR (400 MHz, $CDCl_3$) δ 8.61–8.60 (d, J = 4.4 Hz, 1H), 8.21 (s, 1H), 7.94–7.92 (t, J = 8.4 Hz, 3H), 7.81–7.79 (d, J = 7.6 Hz, 1H), 7.50 (s, 1H), 7.41–7.38 (m, 1H), 7.22–7.20 (d, J = 8.4 Hz, 2H), 7.05 (s, 1H), 4.44 (s, 2H), 3.82 (s, 3H), 3.35 (s, 1H), 3.33 (s, 6H), 3.07 (s, 4H), 2.62 (s, 3H), 2.47 (s, 3H); HRMS (ESI-TOF) m/z for $C_{30}H_{35}N_4O_6S_2$ $[M+H]^+$ calcd 611.1998, found 611.1985. Anal. Calcd for $C_{30}H_{34}N_4O_6S_2$: C, 59.00; H, 5.61; N, 9.17. Found: C, 58.88; H, 5.60; N, 9.19.

4.1.15. 3-(4-Methanesulfonyl-phenoxy)-*N*-(4-{[(2-methoxy-ethyl)-methyl-amino]-methyl}-thiazol-2-yl)-5-(3-methyl-pyridin-2-yl)-benzamide (18e)

45% yield, white solid. ^{1}H NMR (400 MHz, $CDCl_3$) δ 8.48–8.47 (q, J = 6.0 Hz, 1H), 7.97 (s, 1H), 7.88–7.85 (q, J = 8.8 Hz, 2H), 7.68–7.67 (t, J = 3.6 Hz, 1H), 7.58–7.56 (q, J = 8.0 Hz, 1H), 7.44–7.43 (q, J = 3.6 Hz, 1H), 7.20–7.11 (m, 3H), 6.75 (s, 1H), 3.54 (s, 2H), 3.48–3.45 (t, 2H), 3.28 (s, 3H), 3.01 (s, 3H), 2.68–2.59 (t, J = 11.2 Hz, 2H), 2.35 (s, 3H), 2.22 (s, 3H); HRMS (ESI-TOF) m/z for $C_{28}H_{31}N_4O_5S_2$ $[M+H]^+$ calcd 567.1736, found 567.1743. Anal. Calcd for $C_{28}H_{30}N_4O_5S_2$: C, 59.35; H, 5.34; N, 9.89. Found: C, 59.22; H, 5.35; N, 9.91.

4.1.16. 3-(4-Methanesulfonyl-phenoxy)-5-(3-methyl-pyridin-2-yl)-*N*-(4-piperazin-1-ylmethyl-thiazol-2-yl)-benzamide (18f)

40% yield, white solid. ^{1}H NMR (400 MHz, $CDCl_3$) δ 8.47–8.46 (q, J = 5.6 Hz, 1H), 7.91–7.85 (m, 3H), 7.63–7.63 (t, J = 3.6 Hz, 1H), 7.57–7.55 (q, J = 8.0 Hz, 1H), 7.43–7.42 (q, J = 4.0 Hz, 1H), 7.19–7.17 (m, 1H), 7.13–7.10 (q, J = 8.8 Hz, 2H), 6.72 (s, 1H), 3.44 (s, 2H), 3.01 (s, 4H), 2.87–2.84 (t, J = 9.2 Hz, 4H), 2.41 (s, 4H), 2.33 (s, 3H); HRMS (ESI-TOF) m/z for $C_{28}H_{30}N_5O_4S_2$ $[M+H]^+$ calcd 564.1740, found 564.1733. Anal. Calcd for $C_{28}H_{29}N_5O_4S_2$: C, 59.66; H, 5.19; N, 12.42. Found: C, 59.58; H, 5.20; N, 12.45.

4.1.17. 3-(4-Methanesulfonyl-phenoxy)-*N*-{4-[(2-methoxy-1-methyl-ethylamino)-methyl]-thiazol-2-yl}-5-(3-methyl-pyridin-2-yl)-benzamide (18g)

52% yield, white solid. ^{1}H NMR (400 MHz, $CDCl_3$) δ 8.52–8.51 (d, J = 4.4 Hz, 1H), 8.09 (s, 1H), 7.91–7.89 (d, J = 8.8 Hz, 2H), 7.81 (s, 1H), 7.72–7.70 (d, J = 7.6 Hz, 1H), 7.37 (s, 1H), 7.32–7.29 (m, 1H), 7.17–7.15 (d, J = 8.4 Hz, 2H), 6.83 (s, 1H), 4.13 (s, 2H), 3.58–3.56 (d, J = 6.0 Hz, 2H), 3.49–3.44 (m, 1H), 3.29 (s, 3H), 3.06 (s, 3H), 2.61 (s, 3H), 2.39 (s, 3H); HRMS (ESI-TOF) m/z for $C_{28}H_{31}N_4O_5S_2$ $[M+H]^+$ calcd 567.1736, found 567.1736. Anal. Calcd for $C_{28}H_{30}N_4O_5S_2$: C, 59.35; H, 5.34; N, 9.89. Found: C, 59.27; H, 5.36; N, 9.91.

4.1.18. *N*-{4-[(2,2-Dimethoxy-ethylamino)-methyl]-thiazol-2-yl}-3-(4-methanesulfonyl-phenoxy)-5-(3-methyl-pyridin-2-yl)-benzamide (18h)

75% yield, white solid. ^{1}H NMR (400 MHz, MeOD) δ 8.70–8.69 (d, J = 4.8 Hz, 1H), 8.43–8.41 (d, J = 8.0 Hz, 1H), 8.12 (s, 1H), 8.01–7.98 (m, 3H), 7.66–7.66 (t, J = 3.2 Hz, 1H), 7.35–7.30 (m, 3H), 4.66–4.63 (t, J = 8.8 Hz, 3H), 4.26 (s, 2H), 3.44 (s, 6H), 3.19–3.18 (d, J = 4.8 Hz, 2H), 3.12 (s, 3H), 2.49 (s, 3H); HRMS (ESI-TOF) m/z for $C_{28}H_{31}N_4O_6S_2$ $[M+H]^+$ calcd 583.1685, found 583.1679. Anal. Calcd for $C_{28}H_{30}N_4O_6S_2$: C, 57.72; H, 5.19; N, 9.61. Found: C, 57.59; H, 5.18; N, 9.64.

4.1.19. *N*-[4-(Isopropylamino-methyl)-thiazol-2-yl]-3-(4-methanesulfonyl-phenoxy)-5-(3-methyl-pyridin-2-yl)-benzamide (18i)

65% yield, white solid. ^{1}H NMR (400 MHz, $CDCl_3$) δ 8.58–8.57 (d, J = 4.8 Hz, 1H), 8.12 (s, 1H), 7.92–7.90 (d, J = 8.4 Hz, 2H), 7.86–7.82 (m, 2H), 7.42–7.37 (m, 2H), 7.20–7.18 (d, J = 8.4 Hz, 2H), 6.74 (s, 1H), 3.95 (s, 2H), 3.37–3.35 (m, 1H), 3.07 (s, 3H), 2.62 (s, 6H), 2.41 (s, 3H);

HRMS (ESI-TOF) m/z for $C_{27}H_{29}N_4O_4S_2$ $[M+H]^+$ calcd 537.1630, found 537.1637. Anal. Calcd for $C_{27}H_{28}N_4O_4S_2$: C, 60.43; H, 5.26; N, 10.44. Found: C, 60.37; H, 5.24; N, 10.47.

4.1.20. 3-(4-Methanesulfonyl-phenoxy)-5-(3-methyl-pyridin-2-yl)-*N*-(4-prop-2-ynylaminomethyl-thiazol-2-yl)-benzamide (18j)

54% yield, white solid. ^{1}H NMR (400 MHz, $CDCl_3$) δ 8.56–8.55 (d, J = 4.4 Hz, 1H), 8.10 (s, 1H), 7.93–7.91 (d, J = 8.8 Hz, 2H), 7.85 (s, 1H), 7.76–7.74 (d, J = 7.6 Hz, 1H), 7.44 (s, 1H), 7.35–7.35 (m, 1H), 7.20–7.18 (d, J = 8.8 Hz, 2H), 6.79 (s, 1H), 4.17 (s, 2H), 3.83 (s, 2H), 3.14–3.11 (m, 1H), 3.07 (s, 3H), 2.42 (s, 3H); HRMS(ESI-TOF) m/z for $C_{27}H_{25}N_4O_4S_2$ $[M+H]^+$ calcd 533.1317, found 533.1322. Anal. Calcd for $C_{27}H_{24}N_4O_4S_2$: C, 60.89; H, 4.54; N, 10.52. Found: C, 60.80; H, 4.55; N, 10.55.

4.1.21. 3-(4-Methanesulfonyl-phenoxy)-5-(3-methyl-pyridin-2-yl)-*N*-(4-propylaminomethyl-thiazol-2-yl)-benzamide (18k)

70% yield, white solid. ^{1}H NMR (400 MHz, $CDCl_3$) δ 9.44 (br s, 1H), 8.61–8.60 (d, J = 4.8 Hz, 1H), 8.12 (s, 1H), 7.94–7.87 (m, 4H), 7.51–7.48 (t, J = 12.8 Hz, 1H), 7.36 (s, 1H), 7.20–7.18 (d, J = 8.4 Hz, 2H), 6.83 (s, 1H), 3.99 (s, 2H), 3.07 (s, 3H), 2.91–2.87 (m, 2H), 2.62 (s, 3H), 2.42 (s, 3H), 1.74–1.67 (dd, J = 7.6 Hz, 7.6 Hz, 2H); HRMS (ESI-TOF) m/z for $C_{27}H_{29}N_4O_4S_2$ $[M+H]^+$ calcd 537.1630, found 537.1624. Anal. Calcd for $C_{27}H_{28}N_4O_4S_2$: C, 60.43; H, 5.26; N, 10.44. Found: C, 60.36; H, 5.27; N, 10.47.

4.1.22. 3-(4-Methanesulfonylphenoxy)-*N*-(1-methyl-1*H*-pyrazol-3-yl)-5-(3-methylpyridin-2-yl)-benzamide (19a)

To a solution of **13** (187 mg, 0.49 mmol) in dichloromethane (5 mL) were added 1-methyl-1*H*-pyrazol-3-ylamine (71 mg, 0.73 mmol), HOBT (132 mg, 0.98 mmol), EDAC (188 mg, 0.98 mmol) and TEA (0.14 mL, 0.98 mmol) and the reaction mixture was stirred at room temperature overnight. The reaction mixture was then washed with 1 N HCl aqueous solution, saturated $NaHCO_3$ aqueous solution and brine. The organic layer was dried over $MgSO_4$, filtered and concentrated under reduced pressure, and purified by flash column chromatography (EA/*n*-Hex = 1:2 $\sim$ 2:1) to yield 79 mg (35% yield) of **19a** as a white solid. ^{1}H NMR (400 MHz, $CDCl_3$) δ 8.72 (s, 1H), 8.54–8.53 (d, J = 4.4 Hz, 1H), 7.98–7.88 (m, 3H), 7.66–7.61 (m, 2H), 7.45 (s, 1H), 7.28–7.23 (m, 1H), 7.19–7.16 (m, 2H), 6.80 (s, 1H), 3.79 (s, 3H), 3.07 (s, 3H), 2.38 (s, 3H); HRMS (ESI-TOF) m/z for $C_{24}H_{23}N_4O_4S$ $[M+H]^+$ calcd 463.1440, found 463.1425; TLC R_f 0.20(33% *n*-Hx in EtOAc). Anal. Calcd for $C_{24}H_{22}N_4O_4S_2$: C, 62.32; H, 4.79; N, 12.11. Found: C, 62.38; H, 4.77; N, 12.14.

The following compounds **(19b–e)** were prepared according to the procedure described for the synthesis of **19e** using appropriate pyrazoles.

4.1.23. *N*-(1-Ethoxymethyl-1*H*-pyrazol-3-yl)-3-(4-methanesulfonylphenoxy)-5-(3-methylpyridin-2-yl)-benzamide (19b)

52% yield, white solid. ^{1}H NMR (400 MHz, $CDCl_3$) δ 8.91 (s, 1H), 8.55–8.54 (d, J = 5.2 Hz, 1H), 7.95–7.93 (d, J = 8.4 Hz, 1H), 7.85 (s, 1H), 7.69–7.64 (m, 3H), 7.56–7.53 (t, 1H), 7.48–7.44 (m, 2H), 7.21–7.18 (d, J = 8.8 Hz, 1H), 6.72 (s, 1H), 5.54 (s, 2H), 3.62–3.57 (dd, J = 6.8, 6.8 Hz, 2H), 3.07 (s, 3H), 2.41 (s, 3H); HRMS (ESI-TOF) m/z for $C_{26}H_{27}N_4O_5S$ $[M+H]^+$ calcd 507.1702, found 507.1692. Anal. Calcd for $C_{26}H_{26}N_4O_5S$: C, 61.65; H, 5.17; N, 11.06. Found: C, 61.57; H, 5.16; N, 11.09.

4.1.24. *N*-[1-(2-Diethylaminoethyl-1*H*-pyrazol-3-yl)-3-(4-methanesulfonylphenoxy)-5-(3-methylpyridin-2-yl)-benzamide (19c)

50% yield, white solid. ^{1}H NMR (400 MHz, MeOD) δ 8.47–8.46 (d, J = 4.4 Hz, 1H), 8.01–7.97 (d, J = 8.8 Hz, 1H), 7.93 (s, 1H), 7.83–7.81 (d, J = 7.2 Hz, 1H), 7.75 (s, 1H), 7.51 (s, 2H), 7.41–7.39 (t, J = 7.6 Hz, 1H), 7.28 (s, 2H), 6.40 (s, 1H), 4.29–4.26 (t, J = 7.2 Hz, 2H), 3.12 (s, 3H), 2.65 (s, 6H), 2.38 (s, 3H), 1.00 (s, 6H); HRMS (ESI-TOF) m/z for $C_{29}H_{34}N_5O_4S$ $[M+H]^+$ calcd 548.2332, found 548.2321. Calcd for $C_{29}H_{33}N_5O_4S$: C, 66.60; H, 6.07; N, 12.79. Found: C, 66.50; H, 6.06; N, 12.77.

4.1.25. 3-(4-Methanesulfonylphenoxy)-5-(3-methylpyridin-2-yl)-*N*-[1-(2-morpholin-4-yl)-ethyl]-1*H*-pyrazol-3-yl]-benzamide (19d)

53% yield, white solid. ^{1}H NMR (400 MHz, $CDCl_3$) δ 8.55–8.54 (d, J = 4.8 Hz, 1H), 8.44 (s, 1H), 7.94–7.92 (d, J = 8.4 Hz, 2H), 7.88 (s, 1H), 7.66–7.62 (m, 2H), 7.45 (s, 1H), 7.40 (s, 1H), 7.19–7.17 (d, J = 8.8 Hz, 2H), 6.80 (s, 1H), 4.14–4.11 (t, J = 13.2 Hz, 2H), 3.70–3.67 (t, J = 9.2 Hz, 2H), 3.07 (s, 3H), 2.78–2.75 (m, 2H), 2.47–2.45 (t, J = 8.8 Hz, 2H), 2.39 (s, 3H); HRMS (ESI-TOF) m/z for $C_{29}H_{32}N_5O_5S$ $[M+H]^+$ calcd 562.2124, found 562.2131. Anal. Calcd for $C_{29}H_{31}N_5O_5S$: C, 62.02; H, 5.56; N, 12.47. Found: C, 61.96; H, 5.54; N, 12.50.

4.1.26. 3-(4-Methanesulfonylphenoxy)-*N*-[1-(2-methoxyethoxymethyl)-1*H*-pyrazol-3-yl]-5-(3-methylpyridin-2-yl)-benzamide (19e)

To a solution of **13** (2.2 g, 5.74 mmol) in DMF (20 mL) were added 1-(2-methoxyethoxymethyl)-3-amino-1*H*-pyrazole (1.2 g, 7.01 mmol), HATU (3.27 g, 8.60 mol) and DIEA (1.48 g, 11.5 mmol) and the reaction mixture was stirred at room temperature overnight. The reaction mixture was then washed with 1 N HCl aqueous solution, saturated $NaHCO_3$ aqueous solution, and brine. The organic layer was dried over $MgSO_4$, filtered and concentrated under reduced pressure, and purified by flash column chromatography (EA/Pet.Ether = 2:1 $\sim$ 1:1) to afford 1.8 g (75% yield) of **19e** as a white solid. ^{1}H NMR (400 MHz, $CDCl_3$) δ 8.66 (s, 1H), 8.55 (s, 1H), 7.94–7.92 (d, J = 8.4 Hz, 2H), 7.89 (s, 1H), 7.65–7.62 (br s, 2H), 7.52 (s, 1H), 7.45 (s, 1H), 7.26 (s, 1H), 7.19–7.17 (d, J = 8.4 Hz, 2H), 6.92 (s, 1H), 5.39 (s, 2H), 3.61 (s, 2H), 3.51–3.50 (br s, 2H), 3.36 (s, 3H), 3.07 (s, 3H), 2.39 (s, 3H); HRMS (ESI-TOF) m/z for $C_{27}H_{29}N_4O_6S$ $[M+H]^+$ calcd 537.1808, found 537.1799; TLC R_f 0.35 (50% EtOAc in petroleum ether). Anal. Calcd for $C_{27}H_{28}N_4O_6S$: C, 60.43; H, 5.26; N, 10.44. Found: C, 60.36; H, 5.27; N, 10.47.

4.2. Molecular docking

A docking study was carried out using standard protocols with a Surflex-Dock[35] module in SYBYL-X 2.0 (Tripos Inc, St. Louis, MO, USA) modeling package. The crystal structure of glucokinase was retrieved from the RCSB Protein Data Bank (PDB entry code: 3A0I).[27] According to the protocol of Surflex-Dock, substructures including glucose, sodium ion, and water were deleted from the crystal structure modeling and the ligand substructure of the active site was extracted. The glucokinase protein structure was prepared by repairing the backbone and side chains. Hydrogen atoms were then added to the protein structure and ligand. Atom types and charges were also assigned using AMBER7 FF99 force field for protein and Gasteiger–Huckel charge for the ligand. With a standard staged energy minimization protocol, the glucokinase structure was generated with energy minimization using AMBER7 F99 force field with the Powell energy minimization algorithm. Using the extracted ligand, a 'protomol' which is a representation of an idealized ligand to which putative ligands can be aligned, was generated. To predict the appropriate binding conformation for glucokinase activators, co-crystallized ligand was used as a template reference molecule. Docking simulations of compounds were conducted with binding to the active site of glucokinase by an empirical scoring function to score the ligand and

protomol-guided docking in Surflex-Dock. CScore calculations of the docking ligands were also performed.

4.3. Bioassays

For experiments involving the use of animals, all procedures were carried out in accordance with the guidelines of the Institutional Animal Care and Use Committee of Yuhan Research Institute.

4.3.1. Glucokinase enzymatic assay

An enzymatic glucokinase assay using purified recombinant human pancreatic glucokinase was used to evaluate the compounds. Glucokinase activity was assessed spectrometrically by a coupled reaction with glucose-6-phosphate dehydrogenase (G6PDH).[33] Briefly, GK catalyzes glucose phosphorylation to generate glucose-6-P, which is oxidized by G6PDH with the concomitant reduction of NADPH. The resultant NADPH is then monitored via an increase in the rate of absorbance at 340 nm using a plate reader (Spectra-Max 384 plus, Molecular Devices, CA, USA). All compounds were prepared in DMSO and the assay was performed in 96-well plates in a final volume of 100 μL containing 25 mM HEPES pH 7.4, 10 mM glucose, 25 mM KCl, 1 mM $MgCl_2$, 1 mM DTT, 1 mM ATP, 1 mM NADP, 2.5 U/mL G6PDH, 1 mM glucose, 0.1 μg glucokinase, and the test compounds. The fold activation of the enzyme was assessed by comparing with controls (GK activation in DMSO only was considered as 100%). For EC_{50} determination, 12 different concentrations of the compounds were tested in the assay, and the fold changes in activity versus controls were fitted to a sigmoidal curve using a dose–response variable slope model in GraphPad Prism 5.

4.3.2. Glucose uptake in rat primary hepatocytes

Hepatocytes were isolated by in situ liver perfusion with collagenase. The viability of isolated hepatocytes were determined to be over 85% via Trypan blue exclusion assay. Cells were suspended in MEM supplemented with 10% fetal bovine serum (v/v), 100 U/mL penicillin, and 100 μg/mL streptomycin. 1×10^6 cells/well were planted onto collagen 1-coated 12-well plates. After 36 h incubation (37 °C; 5% CO_2/95% air v/v) to allow cell attachment, the medium was replaced with serum-free media for a further 12 h culture. 2-Deoxy-D-[^{3}H]-glucose uptake was assessed in cultured hepatocytes. Cells were washed and incubated in serum-free MEM containing 5.5 mM glucose, and 2 μCi/mL 2-deoxy-D-[^{3}H]-glucose with or without the test compounds for 4 h. The reaction was terminated and washed three times with ice-cold phosphate buffered saline (PBS), and then cells were lysed with 0.1 N NaOH. Portions of cell lysates were used for scintillation counting, and the results were recorded as increased percentage versus control.

4.3.3. Insulin secretion in rat pancreatic islets

An insulin secretion assay was performed using pancreatic islets isolated from male Sprague–Dawley rats. Insulin release was determined during static islet incubation. Briefly, groups of five islets were placed in incubation wells. After a 30-min pre-incubation with HEPES-buffered Krebs–Ringer buffer (pH 7.4) containing 5 mm glucose, islets were transferred to wells containing 2 mL HEPES-buffered Krebs–Ringer buffer and varying concentrations of glucose and the test compounds. The studies were performed at 37 °C in a waterbath shaker with an atmosphere of 5% CO_2. Samples of incubation buffer were collected at 1 h for insulin determination using a mouse ELISA kit (Mercodia, Uppsala, Sweden). Results were recorded as the increased percentage versus control.

4.3.4. In vivo oral glucose tolerance test (OGTT) assay

Anti-diabetic effects of the compounds were evaluated by a glucose tolerance test (OGTT) using normal and diabetic db/db mice. Eight-week old male C57BL/6 mice (OrientBio Inc, Republic of Korea) or ten-week old male C57BLKS/J db/db mice (SLC Inc, Japan) were fasted overnight (with free access to water) before performing the test. The mice were orally administered with the compound or vehicle alone (0.5% methylcellulose solution). After 30 min, the mice were administered with an oral glucose challenge (2 g/kg). Blood glucose concentrations were measured by GlucoDr AMG-3000 (Allmedicus Inc., Republic of Korea) just prior to and following the glucose challenge (30, 60, 90, 120 and 180 min) from the tail tip. AUC values of the time–glucose curve were calculated from the data.

4.4. Measurement of physiochemical properties

Aqueous solubility of the compounds in phosphate buffer (pH 7.4) was determined. To investigate permeability of the compounds, the $P_{app,\ PAMPA}$ values (via parallel artificial membrane permeability assay (PAMPA)) were measured experimentally using a BD Gentest™ Pre-coated PAMPA Plate System. In vitro metabolism studies for CYP inhibition and time-dependent inhibition (TDI) were performed using human liver microsomes and incubation conditions were similar to those previously described.[34] Briefly, the incubation mixtures containing pooled human liver microsomes (0.25 mg/mL), CYP-selective substrates, and each test compound (up to 25 μM) were preincubated at 37 °C. The reaction was initiated by adding an NADPH-generating system (1.3 mM NADP, 3.3 mM glucose 6-phosphate, 3.3 mM $MgCl_2$, and 1.0 unit/mL glucose-6-phosphate dehydrogenase). After incubation, the reaction was stopped by placing the tubes on ice and adding ice-cold acetonitrile solution. The incubation mixtures were then centrifuged (10,000*g* for 5 min at 4 °C). Supernatant aliquots were injected into an LC–MS/MS system.

4.5. Pharmacokinetics (PK) protocol

ICR male mice and SD rats (7-weeks old) received an intravenous bolus (3 mg/kg) and oral gavage doses (10 mg/kg) of the test compound. Blood samples were obtained at 0.08 (iv only), 0.25, 0.5, 1, 2, 4, and 7 h after drug administration. Plasma samples were obtained following centrifugation of blood at 4 °C and stored at −20 °C for analysis. To a 0.1 mL aliquot of mouse or rat plasma, 0.2 mL of acetonitrile was added. The mixture was vortexed for 10 min and then centrifuged for a further 10 min. The supernatant was then tested for test compound concentration via HPLC. Pharmacokinetic variables were evaluated by noncompartmental analysis using WinNonlin Professional Version 5.2 (Pharsight, MO, USA).

4.6. Toxicity study

4.6.1. 14-Day repeated oral dose toxicity study in rats

Specific pathogen-free Sprague–Dawley rats of each gender (20 males and 20 females) at 5 weeks of age were obtained from ORIENTBIO INC. (Republic of Korea). These animals were housed in a room maintained at a temperature of 22 ± 2 °C and a relative humidity of 50 ± 15%, with artificial lighting from 08:00 to 20:00 (150–300 Lux) and 10–15 air changes per hour. Each animal was housed in separate stainless steel cages (W260 × D350 × H210 mm). All rats had free access to tap water and food (Teklad Certified Irradiated Global 18% Protein Rodent Diet 2918C, Harlan Laboratories Inc., USA). Male and female rats were assigned to Groups 1 through 4 and the compound was administered at dose levels of 0, 250, 500, and 1000 mg/kg body weight/day (mg/kg/day) for 14 days. Group 1 received vehicle control (0.5% methylcellulose solution) and animals were dosed at a volume of 10 mL/kg. After 14 days of treatment, all surviving animals were sacrificed and necropsied by Day 15. Liver from each animal

was preserved in 10% neutral-buffered formalin and testis was preserved in modified Davidson's fixative. The tissue was embedded in paraffin wax, sectioned, stained with hematoxylin and eosin (H&E) and examined microscopically. Histopathological examination was performed only on control and high-dose groups of both genders.

4.6.2. Escalating oral gavage dose range-finding study in beagle dogs

Male and female beagle dogs (1 each) were obtained from Marshall Biotech. Co., Ltd (Beijing, China). The dogs were 5 months old and weighed 6.1 kg (male) and 5.98 kg (female) at the initiation of the study. Dogs were acclimated to laboratory conditions for 14 days, and were housed in stainless steel cages in a room maintained at 23 ± 3 °C and a relative humidity of 28–67%, with artificial lighting from 08:00 to 20:00 (150–300 Lux) and 10–15 air changes per hour. All dogs were fed Purina Certified Lab Canine Diet (Agribrands Purina Korea Inc.) with filtered tap water available *ad libitum*. Animals were administered with the test compound at repeated escalating dose levels of 100, 300, and 1000 mg/kg of body weight/day (mg/kg/day) for 8 days (at Days 3, 6, and 8 for each dose). The vehicle control was 0.5% methylcellulose solution and the animals were dosed at a volume of 5 mL/kg. Necropsies were performed on the two animals at the termination of the study. Test is were preserved in modified Davidson's fixative. The tissue was embedded in paraffin wax, sectioned, stained with hematoxylin and eosin (H&E), and examined microscopically.

4.6.3. Mutagenicity study

Mutagenicity testing was carried out according to standard Ames test procedures (Maron and Ames). Two *Salmonella typhimurium* strains (TA98 and TA100) were used in a reverse mutation test both with and without S9 mix (Aroclor 1254-induced male Sprague–Dawley rat liver (MOLTOX™, USA) and Cofactor-I (Wako Chemicals, Japan). The designated **19e** concentrations in this test were 1.5, 5, 15, 50, 150, 500, 1500, 5000 μg/plate. The treatment mixture and plate conditions were checked for the formation of precipitation and cytotoxicity and the test strains were exposed using a direct plate incorporation method. A small amount of bacterial growth on each master plate was transferred to a flask containing 20 mL of liquid medium (2.5% Oxoid Nutrient Broth No.2). Inoculated flasks were incubated for 10 h in a shaker/incubator (37 ± 2 °C, 120 rpm). Viable cell counts from overnight cultures were determined by optical densitometry (OD) at 600 nM, and the cultures were stored at 4 °C. For the plating assay, 0.5 mL of S9 mix, 0.1 mL of bacterial culture and 0.1 mL of **19e** dissolved in DMSO were added to each sterile culture tube containing 2 mL of top agar held at 45 ± 2 °C in a dry bath. After the top agar solidified, plates were inverted and incubated at 37 ± 2 °C for 50 ± 2 h and then revertant colonies were counted. For cultures without S9 mix, sodium azide (0.5 μg/plate) and 4-nitroquinoline-N-oxide (0.5 g/plate) were used as positive controls for TA100 and TA98, respectively. In cultures containing S9 mix, 2-aminoanthracene (1 μg/plate) for TA100 and benzo[*a*]pyrene (1 μg/plate) for TA98 were used as positive controls. The evaluation criteria defined a positive result as reproducible exhibiting a more than 2 fold dose-related increase in the number of revertants per plate in at least one strain with or without a metabolic activation system.

Acknowledgements

This study was supported by a Grant from the Chungcheong Leading Industry Office for Medicine & Bio Projects, Ministry of Knowledge Economy, Republic of Korea (C-2-1, 500108, 7007618). The authors would like to thank Professor Woo-Chan Son at the University of Ulsan College of Medicine and Professor Hee-Sook Jun at Gachon University of Medicine & Science for their helpful discussion. We also thank Lee Farrand for proofreading the manuscript.

References and notes

1. Fowler, M. J. *Clin. Diab.* **2008**, *26*, 77.
2. Kahn, S. E.; Hull, R. L.; Utzschneider, K. M. *Nature* **2006**, *444*, 840.
3. Bouchie, A. *Nat. Biotechnol.* **2013**, *31*, 469.
4. Han, S.; Hagan, D. L.; Taylor, J. R.; Xin, L.; Meng, W.; Biller, S. A.; Wetterau, J. R.; Washburn, W. N.; Whaley, J. M. *Diabetes* **2008**, *57*, 1723.
5. Stenlöf, K.; Cefalu, W. T.; Kim, K. A.; Alba, M.; Usiskin, K.; Tong, C.; Canovatchel, W.; Meininger, G. *Diabetes Obes. Metab.* **2013**, *15*, 372.
6. *Joslin's Diabetes Mellitus*; Lebovitz, H. E., Ed., 14th ed.; Lippincott Williams & Wilkins: Philadelphia, PA, 2005; p 687.
7. Ralph, E. C.; Thomson, J.; Almaden, J.; Sun, S. *Biochemistry* **2008**, *47*, 5028.
8. Matschinsky, F. M. *Diabetes* **1996**, *45*, 223.
9. Antoine, M.; Boutin, J. A.; Ferry, G. *Biochemistry* **2009**, *48*, 5466.
10. Heredia, W.; Thomson, J.; Nettleton, D.; Sun, S. *Biochemistry* **2006**, *45*, 7553.
11. Matschinsky, F. M.; Glaser, B.; Magnuson, M. A. *Diabetes* **1998**, *47*, 307.
12. Waring, M. J.; Brogan, I. J.; Coghlan, M.; Johnstone, C.; Jones, H. B.; Leighton, B.; Mckerrecher, D.; Pike, K. G.; Robb, G. R. *Med. Chem. Commun.* **2011**, *2*, 771.
13. Pfefferkorn, J. A.; Guzman-Perez, A.; Oates, P. J.; Litchfield, J.; Aspnes, G.; Basak, A., et al *Med. Chem. Commun.* **2011**, *2*, 828.
14. Pfefferkorn, J. A.; Guzman-Perez, A.; Litchfield, J.; Aiello, R.; Treadway, J. L.; Pattersen, J.; Minich, M. L.; Filipski, K. J.; Jones, C. S.; Tu, M.; Aspnes, G.; Sweet, L.; Liras, S.; Rolph, T. P., et al *J. Med. Chem.* **2012**, *55*, 1318.
15. Massa, M. L.; Gagliardino, J. J.; Francini, F. *Life* **2011**, *63*, 1.
16. Bebernitz, G. R.; Beaulieu, V.; Dale, B. A.; Deacon, R.; Duttaroy, A.; Gao, J.; Grondine, M. S.; Gupta, R. C.; Kakmak, M.; Kavana, M.; Kirman, L. C.; Liang, J.; Maniara, W. M.; Munshi, S.; Nadkarni, S. S.; Schuster, H. F.; Stams, T.; St Denny, I.; Taslimi, P. M.; Vash, B.; Caplan, S. L. *J. Med. Chem.* **2009**, *52*, 6142.
17. Park, K.; Lee, B.-M.; Kim, Y.-H.; Han, T.; Yi, W.; Lee, D.-H.; Choi, H.-H.; Chong, W.; Lee, C.-H. *Bioorg. Med. Chem. Lett.* **2013**, *23*, 537.
18. Park, K. *Arch. Pharmacal Res.* **2012**, *35*, 2029.
19. Matschinsky, F. M. *Trends Pharmacol. Sci.* **2013**, *34*, 90.
20. Verspohl, E. J. *Pharmacol. Rev.* **2012**, *2*, 188.
21. Winzell, M. S.; Coghlan, M.; Leighton, B.; Frangioudakis, G.; Smith, D. M.; Storlien, L. H.; Ahrén, B. *Eur. J. Pharmacol.* **2011**, *663*, 80.
22. (a) Fyfe, M. C. T.; Procter, M. J. *Drugs Future* **2009**, *34*, 641; (b) Matschinsky, F. *Nat. Rev. Drug Disc.* **2009**, *8*, 399.
23. Iino, T.; Hashimoto, N.; Hasegawa, T.; Chiba, M.; Eiki, J.; Nishimura, T. *Bioorg. Med. Chem. Lett.* **2010**, *20*, 1619.
24. Sidduri, A.; Grimsby, J. S.; Corbett, W. L.; Sarabu, R.; Grippo, J. F.; Lou, J.; Kester, R. F.; Dvorozniak, M.; Marcus, L.; Spence, C.; Racha, J. K.; Moore, D. J. *Bioorg. Med. Chem. Lett.* **2010**, *20*, 5673.
25. Grimsby, J.; Sarabu, R.; Corbett, W. L.; Hayne, N. E.; Bizzarro, F. T.; Coffey, J. W.; Guertin, K. R.; Hilliard, D. W.; Kester, R. F.; Mahaney, P. E.; Marcus, L.; Qi, L. D.; Soence, C. L.; Tengi, J.; Magnuson, M. A.; Chu, C. A.; Dvorozniak, M. T.; Matschinsky, F. M.; Grippo, J. F. *Science* **2003**, *301*, 370.
26. Sarabu, R.; Tilley, J. W.; Grimsby, J. *RSC Drug Discov. Series* **2011**, *4*, 51.
27. Mitsuya, M.; Kamata, K.; Bamba, M.; Watanabe, H.; Sasaki, Y.; Sasaki, K.; Ohyama, S.; Hosaka, H.; Nagata, Y.; Eiki, J.; Nishimura, T. *Bioorg. Med. Chem. Lett.* **2009**, *19*, 2718.
28. Waring, M. J.; Johnstone, C.; McKerrecher, D.; Pike, K. G.; Robb, G. R. *Med. Chem. Commun.* **2011**, *2*, 775.
29. Meininger, G. E.; Scott, R.; Alba, R.; Shentu, Y.; Luo, E.; Amin, H.; Davies, M. J.; Kaufman, K. D.; Goldstein, B. J. *Diabetes Care* **2011**, *34*, 2560.
30. Pike, K. G.; Allen, J. V.; Caulkett, P. W.; Clarke, D. S.; Donald, C. S.; Fenwick, M. L.; Johnson, K. M.; Johnstone, C.; McKerrecher, D.; Rayner, J. W.; Walker, R. P.; Wilson, I. *Bioorg. Med. Chem. Lett.* **2011**, *11*, 3467.
31. (a) Iino, T.; Sasaki, Y.; Bamba, M.; Mitsuya, M.; Ohno, A.; Kamata, K.; Hosaka, H.; Maruki, H.; Futamura, M.; Yoshimoto, R.; Ohyama, S.; Sasaki, K.; Chiba, M.; Ohtake, N.; Nagata, Y.; Eiki, J.; Nishimura, T. *Bioorg. Med. Chem. Lett.* **2009**, *19*, 5531; (b) Takahashi, K.; Hashimoto, N.; Nakama, C.; Kamata, K.; Sasaki, K.; Yoshimoto, R.; Ohyama, S.; Hosaka, H.; Maruki, H.; Nagata, Y.; Eiki, J.; Nishimura, T. *Bioorg. Med. Chem.* **2009**, *17*, 7042; (c) Nishimura, T.; Iino, T.; Mitsuya, M.; Bamba, M.; Watanabe, H.; Tsukahara, D.; Kamata, K.; Sasaki, K.; Ohyama, S.; Hosaka, H.; Futamura, M.; Nagata, Y.; Eiki, J. *Bioorg. Med. Chem. Lett.* **2009**, *19*, 1357; (d) Ishikawa, M.; Nonoshita, K.; Ogino, Y.; Nagae, Y.; Tsukahara, D.; Hosaka, H.; Maruki, H.; Ohyama, S.; Yoshimoto, R.; Sasaki, K.; Nagata, Y.; Eiki, J.; Nishimura, T. *Bioorg. Med. Chem. Lett.* **2009**, *19*, 4450; (e) Iino, T.; Hashimoto, N.; Sasaki, K.; Ohyama, S.; Yoshimoto, R.; Hosaka, H.; Hasegawa, T.; Chiba, M.; Nagata, Y.; Eiki, J.; Nishimura, T. *Bioorg. Med. Chem.* **2009**, *17*, 3800.
32. Johnson, D.; Shepherd, R. M.; Gill, D.; Gorman, T.; Smith, D. M.; Dunne, M. J. *Diabetes* **2007**, *56*, 1694.
33. Fyfe, M. C.; White, J. R.; Taylor, A.; Chatfield, R.; Wargent, E.; Printz, R. L.; Sulpice, T.; McCormack, J. G.; Procter, M. J.; Reynet, C.; Widdowson, P. S.; Wong-Kai-In, P. *Diabetologia* **2007**, *50*, 1277.
34. (a) Bae, S. K.; Cao, S.; Seo, K. A.; Kim, H.; Kim, M. J.; Shon, J. H.; Liu, K. H.; Zhou, H. H.; Shin, J. G. *Drug Metab. Dispos.* **2008**, *36*, 1679; (b) Parkinson, A.; Kazmi, F.; Buckley, D. B.; Yerino, P.; Paris, B. L.; Holsapple, J.; Toren, P.; Otradovec, S. M.; Ogilvie, B. W. *Drug Metab. Dispos.* **2011**, *39*, 1370.
35. Jain, A. N. *J. Med. Chem.* **2003**, *46*, 499.